

k FW: A Frank-Wolfe style algorithm with stronger subproblem oracles

Lijun Ding, Jicong Fan, and Madeleine Udell*

November 17, 2021

Abstract

This paper proposes a new variant of Frank-Wolfe (FW), called k FW. Standard FW suffers from slow convergence: iterates often zig-zag as update directions oscillate around extreme points of the constraint set. The new variant, k FW, overcomes this problem by using two stronger subproblem oracles in each iteration. The first is a k linear optimization oracle (k LOO) that computes the k best update directions (rather than just one). The second is a k direction search (k DS) that minimizes the objective over a constraint set represented by the k best update directions and the previous iterate. When the problem solution admits a sparse representation, both oracles are easy to compute, and k FW converges quickly for smooth convex objectives and several interesting constraint sets: k FW achieves finite $\frac{4L_f^3 D^4}{\gamma \delta^2}$ convergence on polytopes and group norm balls, and linear convergence on spectrahedra and nuclear norm balls. Numerical experiments validate the effectiveness of k FW and demonstrate an order-of-magnitude speedup over existing approaches.

1 Introduction

We consider the following optimization problem with decision variable x :

$$\begin{aligned} & \text{minimize} && f(x) := g(\mathcal{A}x) + \langle c, x \rangle \\ & \text{subject to} && x \in \Omega. \end{aligned} \tag{1}$$

The constraint set $\Omega \subseteq \mathbf{E}$ is a convex and compact subset of a finite dimensional Euclidean space \mathbf{E} and has diameter D^1 . The map $\mathcal{A} : \mathbf{E} \rightarrow \mathbf{F}$ is linear, where \mathbf{F} is another finite dimensional Euclidean space. We equip both spaces \mathbf{E} and \mathbf{F} with real inner products denoted as $\langle \cdot, \cdot \rangle$. The vector c is in \mathbf{E} . The function $g : \mathbf{F} \rightarrow \mathbb{R}$ is convex and L_g -smooth². The smoothness of g implies that f is L_f -smooth for some $L_f > 0$. For ease of exposition, we assume Problem (1) admits a unique solution.³

Applications. The optimization problem (1) appears in a wide variety of applications, such as sparse vector recovery [CDS01], group-sparse vector recovery [YL06], combinatorial problems [JTFF14], submodular optimization [B⁺13, ZGU18], and low rank matrix recovery problems [RFP10, JS10, YUTC17, DU18].

*L. Ding is with the Department of Mathematics, University of Washington, Seattle, WA 98195, USA. E-mail: ljdj@uw.edu. Jicong Fan is with the School of Data Science, The Chinese University of Hong Kong, Shenzhen, China. E-mail: fanjicong@cuhk.edu.cn. M. Udell is with the School of Operations Research and Information Engineering, Cornell University, Ithaca, NY 14850, USA. E-mail: udell@cornell.edu.

¹The diameter of Ω is defined as $\sup_{x,y \in \Omega} \|x - y\|$, where $\|\cdot\|$ is the norm induced by the inner product.

²That is, the gradient of g is L_g -Lipschitz continuous with respect to the norm $\|\cdot\|$.

³The main results Theorem 6, 7 and 10 remain valid for multiple optimal solution setting after minor adjustments, see Section C. Note that from [DL11, Corollary 3.5], the solution is indeed unique for almost all c .

Frank-Wolfe and two subproblems. In many modern high-dimensional applications, Euclidean projection onto the set Ω is challenging. Hence the well-known projected gradient (PG) method and its acceleration version (APG) are not well suited for (1). Instead, researchers have turned to projection-free methods, such as the Frank-Wolfe algorithm (FW) [FW56], also known as the conditional gradient method [LP66, Section 6]. As stated in Algorithm 1, FW operates in two computational steps:

1. *Linear Optimization Oracle (LOO):* Find a direction v_t that solves $\min_v \langle \nabla f(x_t), v \rangle$.
2. *Line Search:* Find x_{t+1} that solves $\min_{x=\eta v_t+(1-\eta)x_t, \eta \in [0,1]} f(x)$.

The linear optimization oracle can be computed efficiently for many interesting constraint sets Ω even when projection is prohibitively expensive. These sets include the probability simplex, the ℓ_1 norm ball, and many more polytopes arising from combinatorial optimization, the spectrahedron $\mathcal{SP}^n = \{X \in \mathbb{S}_+^n \mid \text{tr}(X) = 1\}$, and the unit nuclear norm ball $\mathbf{B}_{\|\cdot\|_{\text{nuc}}} = \{X \mid \|X\|_{\text{nuc}} \leq 1\}$. We refer the reader to [Jag13, LJJ15] for further examples. Line search is easy to implement using a closed formula for quadratic f , or bisection in general.

Slow convergence of FW and the Zigzag. However, FW is known to be slow in both theory and practice, reaching an accuracy of $\mathcal{O}(\frac{1}{t})$ after t iterations. This slow convergence is often described pictorially by the *Zigzag phenomenon* depicted in Figure 1a. The Zigzag phenomenon occurs when the optimal solution x_\star of (1) lies on the boundary of Ω and is a convex combination of r_\star many extreme points $v_1^\star, \dots, v_{r_\star}^\star \in \Omega$, (In Figure 1a, $r_\star = 2$.)

$$x_\star = \sum_{i=1}^{r_\star} \lambda_i^\star v_i^\star, \quad \lambda_i^\star > 0, \quad \text{and} \quad \sum_{i=1}^{r_\star} \lambda_i^\star = 1. \quad (2)$$

When Ω is a polytope, the LOO will alternate between the extreme points v_i^\star s and the line search updates the estimate of λ_i^\star slowly as the iterate approaches to x_\star . A similar Zigzag occurs for other sets such as the spectrahedron and nuclear norm ball. A long line of work has explored methods to reduce the complexity of FW using LOO and line search alone [GM86, LJJ13, LJJ15, GH15, GM16, FGM17].

Our key insight: overcoming zigzags with k FW. Our first observation is that the sparsity r_\star is expected to be small for most large scale applications mentioned. For example, the sparsity is the number of nonzeros in sparse vector recovery, the number of nonzero groups in group-sparse vector recovery, and the rank in low rank matrix recovery. Next, note that from the optimality condition (also see Figure 1b), the gradient $\nabla f(x_\star)$ in this case has the smallest inner product with $v_1^\star, \dots, v_{r_\star}^\star$ among all $v \in \Omega$. Also, for small r_\star , we can solve $\min_{x \in \text{conv}(x_t, v_1^\star, \dots, v_{r_\star}^\star)} f(x)$ efficiently⁴ to obtain the solution x_\star . Hence, our key insight to overcome the Zigzag is simply

*Compute all extreme points v_i^\star that minimize $\langle \nabla f(x_\star), v \rangle$
and solve the smaller problem $\min_{x \in \text{conv}(x_t, v_1^\star, \dots, v_{r_\star}^\star)} f(x)$.*

⁴Here $\text{conv}(v_1^\star, \dots, v_{r_\star}^\star)$ is the convex hull of v_1, \dots, v_{r_\star} .

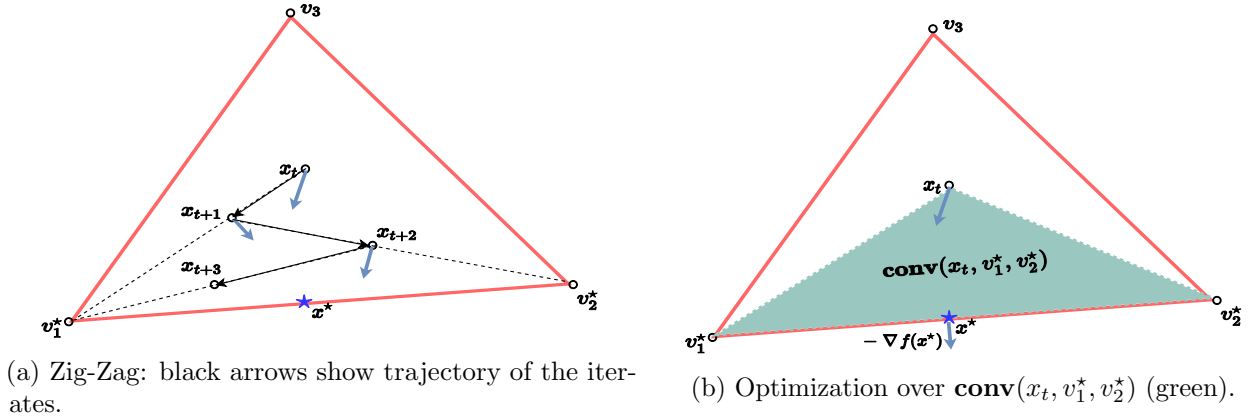


Figure 1: The Zigzag phenomenon and optimization over $\text{conv}(x_t, v_1^*, v_2^*)$. Here, the solution x_* is a convex combination of v_1^* and v_2^* , and $r_* = 2$. The grey arrows are the negative gradients $-\nabla f$.

This insight leads us to define a new algorithmic ways to choose extreme points and define a smaller convex search set, which we call k LOO and k DS. For polytope Ω , they are defined as

- k linear optimization oracle (k LOO): for any $y \in \mathbb{R}^n$, compute the k extreme points v_1, \dots, v_k (k best directions) with the smallest k inner products $\langle v, y \rangle$ among all extreme points v of Ω .
- k direction search (k DS): given input directions $w, v_1, \dots, v_k \in \Omega$, output $x_{k\text{DS}} = \arg \min_{x \in \text{conv}(w, v_1, \dots, v_k)} f(x)$.

In connection with FW, k LOO and k DS can be considered as stronger subproblem oracles compared to LOO and line search respectively.

Combining the two subproblem oracles, we arrive at a new variant of the Frank-Wolfe algorithm: k FW, presented in Algorithm 2. In Section 2, we show that the two subproblems can actually be efficiently solved over many polytopes (for small k). Moreover, we redefine k LOO and k DS to incorporate the situation where k best extreme points are not well-defined for sets such as group norm ball, spectrahedron, and nuclear norm ball, yet sparsity structure still persists. Finally, we note that with our terminology, 1FW is the same as FW. Hence our main results, Theorem 6, 7, and 10, give new insight into the fast convergence of FW when $r_* = 1$.

Computational efficiency of k FW. Here we summarize the computational efficiency of k FW in terms of its per iteration cost, iteration complexity, and storage for polytopes:

- *Per iteration cost:* For many important cases displayed in Section 2, k FW admits efficient subproblem oracles.
- *Iteration complexity:* k FW achieves the same $\mathcal{O}(1/t)$ convergence rate of FW. Under additional regularity conditions, it achieves nonexponential finite convergence over the polytope and group norm ball and linear convergence over the spectrahedron and nuclear norm ball, as shown in Theorem 6, 7, and 10. These convergence results are beyond the reach of FW and many of its variants [GM86, LJJ15, GM16, FGM17].
- *Storage:* The storage required by k FW is $\mathcal{O}(kn)$, needed to store the k best directions computed in each step, while the pairwise step, away step, and fully corrective step based FW [LJJ15] require $\mathcal{O}(\min(tn, n^2))$ storage to accumulate vectors in n -dimensional Euclidean space computed from LOO ⁵.

A comparison of k FW with FW, away-step FW [GM86], and fully corrective FW (FCFW) [Jag13, Algorithm 4] is shown in Table 1. A recent result [Gar20] shows that away-step FW can have better

⁵The algorithmic Caratheodory procedure described by [BS17] can reduce the number of points stored to n .

Table 1: Comparison of k FW, FW, FW with away step, and FCFW for Problem (1), smooth convex optimization over a constraint set Ω in a n -dimensional Euclidean space. We display the per iteration computation (per iter. comp.), storage, faster rate (compared to $\mathcal{O}(\frac{1}{t})$ rate) under the condition on Ω , extra conditions on Problem (1) to achieve the faster rate (Ex. Cond.), and the reference providing the proof of the rate. A recent result [Gar20] shows that away-step FW can have better convergence and storage after a initial burn-in period under similar assumptions as ours. However, it is hard to quantify the burn-in period as it depends on the parameter of the face where the solution lies. Even without the extra conditions listed in the table, all algorithms admit a $\mathcal{O}(\frac{1}{t})$ convergence rate (see [Jag13] and Theorem 6). Here $t \wedge n = \min(t, n)$. Definitions of the sparsity measure r_\star , strict complementarity (str. comp.), and quadratic growth (q.g.) can be found in Section 3.1.

Algorithm	Per iter. comp.	Storage	Rate and Ω Shape	Ex. Cond.	Reference
FW	LOO, 1DS	$\mathcal{O}(n)$	finite polytope, group norm ball	str. comp., q.g., and $r_\star = 1$	Theorem 7
			linear spectrahedron $\mathbf{B}_{\ \cdot\ _{\text{nuc}}}$		Theorem 10
Away-step FW	LOO, 1DS, and $t \wedge n$ inner products	$\mathcal{O}(n(t \wedge n))$	linear polytope	q.g.	[LJJ15],[Gar20]
FCFW	LOO, and $(t \wedge n)$ DS	$\mathcal{O}(n(t \wedge n))$	linear polytope	q.g.	[LJJ15]
k FW	k LOO, and k DS	$\mathcal{O}(kn)$	finite polytope, group norm ball	str. comp., q.g., and $k \geq r_\star$	Theorem 7
			linear spectrahedron $\mathbf{B}_{\ \cdot\ _{\text{nuc}}}$		Theorem 10

convergence and storage property after an initial burn-in period under similar assumptions as ours. Interestingly, in our experiments in Section 4, we did not observe much of the benefit.

Paper Organization. The rest of the paper is organized as follows. In Section 2, we explain how to solve the two subproblems over a polytope Ω , and how to extend the idea to group norm ball, spectrahedron, and nuclear norm ball. In Section 3, we describe a few analytical conditions, and then present the faster convergence guarantees of k FW under these conditions for the polytope, group norm ball, spectrahedron, and nuclear norm ball. We demonstrate the effectiveness of k FW numerically in Section 4. In Section 5, we conclude the paper and present a discussion on related work and future direction is presented.

Notation. The Euclidean spaces of interest in this paper are the n -th dimensional real Euclidean space \mathbb{R}^n , the set of real matrices $\mathbb{R}^{n_1 \times n_2}$, and the set of symmetric matrices \mathbb{S}^n in $\mathbb{R}^{n \times n}$. We equip the first one with the standard dot product and the latter two with the trace inner product. The induced norm is denoted as $\|\cdot\|$ if not specified. For a linear map $\mathcal{B} : \mathbf{E}_1 \rightarrow \mathbf{E}_2$ between two Euclidean spaces, we define its operator norm as $\|\mathcal{B}\|_{\text{op}} = \max_{\|x\| \leq 1} \|\mathcal{B}(x)\|$. We denote the eigenvalues of a symmetric matrix $A \in \mathbb{S}^n$ as $\lambda_1(A) \geq \dots \geq \lambda_n(A)$. The i -th largest singular value of a rectangular matrix $B \in \mathbb{R}^{n_1 \times n_2}$ is denoted as $\sigma_i(B)$. A matrix $A \in \mathbb{S}^n$ is positive semidefinite if all its eigenvalues are nonnegative and is denoted as $A \succeq 0$ or $A \in \mathbb{S}_+^n$. The column space of a matrix A is written as $\text{range}(A)$. The i -th standard basis vector with appropriate dimension is denoted as e_i .

2 Stronger subproblem oracles for polytopes and beyond

In Section 2.1, we explain when the subproblem oracles can be implemented efficiently for polytopes. We then show how to extend k FW to more complex constraint sets by an appropriate definition of k LOO and k DS in Section 2.2.

2.1 Stronger subproblem oracles for polytopes

Let us first explain when the k LOO can be implemented efficiently for a polytope $\Omega \subseteq \mathbb{R}^n$.

Solving k LOO. Computing a LOO can be NP-hard for some constraint sets Ω : for example, the 0-1 knapsack problem can be formulated as linear optimization over an appropriate polytope. Hence we should not expect that we can compute a k LOO efficiently without further assumptions on the polytope $\Omega \subseteq \mathbb{R}^n$. Since many polytopes come from problems in combinatorics, for these polytopes, computing a k LOO is equivalent to computing the k best solutions to a problem in the combinatorics literature, and polynomial time algorithms are available for many polytopes [Mur68, Law72, HQ85, Epp14]. We present the time complexity of computing k LOO for many interesting problems in Table 5 in the appendix.

Efficient k LOO. Unfortunately, for some polytopes, the time required to compute a k LOO grows superlinearly in k even if $k \leq n$. Hence we restrict our attention to special structured polytopes for which the time complexity of k LOO is no more than k times the complexity of LOO.

Our primary example is the probability simplex $\Delta^n = \mathbf{conv}(\{e_i\}_{i=1}^n)$ in \mathbb{R}^n . Since the vertices of Δ^n are the coordinate vectors $e_i, i = 1, \dots, n$, the inner product of vertex e_i with a vector $y \in \mathbb{R}^n$ is $\langle y, e_i \rangle = y_i$. Hence in this case, k LOO with input $y \in \mathbb{R}^n$ simply outputs the coordinate vectors corresponding to the smallest k values of y . Using a binary heap of k nodes, we can scan through the entries of y and update the heap to keep the k smallest entries seen so far and their indices. Since each heap update takes time $\mathcal{O}(\log k)$, the time to compute k LOO is $\mathcal{O}(n \log k)$. A more sophisticated procedure called *quickselect* improves the time to $\mathcal{O}(n + k)$ [MR01], [Epp14, Section 2.1]. Other examples of efficient k LOO includes, the ℓ_1 norm ball, the spanning tree polytope [Epp90], the Birkhoff polytope, [Mur68], and the path polytope of a directed acyclic graph [Epp98]. More details of each example and its application can be found in Section A.2 in the appendix.

Next, we explain how to compute the k direction search.

k direction search. The k direction search problem optimizes the objective $f(x)$ over $x \in \mathbf{conv}(w, v_1, \dots, v_k) = \{\sum_{i=1}^k \lambda_i v_i + \eta w \mid (\eta, \lambda) \in \Delta^{k+1}\}$. We parametrize this set by $(\eta, \lambda) \in \Delta^{k+1}$ and employ the accelerated projected gradient method (APG) to solve

$$\min_{(\eta, \lambda) \in \Delta^{k+1}} f \left(\sum_{i=1}^k \lambda_i v_i + \eta w \right). \quad (3)$$

The constraint set here is a $k + 1$ dimensional probability simplex; projection onto this set requires time $\mathcal{O}(k \log k)$ [CY11]. Hence for small k , we can solve (3) efficiently. We recover the output $x_{k\text{-DS}} = \sum_{i=1}^k \lambda_i^* v_i + \eta^* w$ of k DS from the optimal solution (η^*, λ^*) of (3).

Remark 1. Optimizing over $\mathbf{conv}(w, v_1, \dots, v_k) = \{\sum_{i=1}^k \lambda_i v_i + \eta w \mid (\eta, \lambda) \in \Delta^{k+1}\}$ using the representation (η, λ) can be challenging due to the high dimension k of this parametrization. Here we discuss a few alternative parametrizations that facilitate optimization.

For example, consider the product of simplices $\prod_{j=1}^d \Delta_{k_j} \subset \mathbb{R}^{\sum_{j=1}^d k_j}$, which appears in a variety of applications [LJJP13]. Denote the j -th block of $w \in \mathbb{R}^{\sum_{j=1}^d k_j}$ as $[w]^j \in \mathbb{R}^{k_j}$, and let $e_i^j \in \mathbb{R}^{\sum_{j=1}^d k_j}$ be the indicator of the i -th position in j -th block (1 there, and 0 everywhere else). Write $e_{i_1 \dots i_d} = \sum_{j=1}^d e_{i_j}^j$. Define the set $I = \prod_{j=1}^d I_j$ where $I_j \subset \{1, \dots, k_j\}$, which might be the generated when we apply $|I_j|$ LOO in each block within $\mathcal{O}((\sum_{j=1}^d k_j) \log(\max_j |I_j|))$ time. Suppose we want to optimize over $\mathbf{conv}(w, \{e_{i_1 \dots i_d}\}_{(i_1, \dots, i_d) \in I})$. If we use the (η, λ) representation, the size of (η, λ) is $\prod |I_j| + 1$ which can be much larger than the number of nonzeros, $\sum_{j=1}^d |I_j|$, of the solution x_* or even larger than the total dimension $\sum_{j=1}^d |k_j|$, even if the support of x_* in j -th block is exactly I_j .

To remedy the situation, we can equivalently parametrize the feasible set as convex combinations of w and the indicator vectors e_i^j . Explicitly, consider the set $A_I = \{(\{\alpha_{ij}\}_{1 \leq j \leq d, i \in I_j}, \eta) \mid \alpha_{ij} \geq 0 \forall i, j, \eta \geq 0, \sum_{i \in I_j} \alpha_{ij} + \eta = 1\}$. It is then straightforward to verify that $\mathbf{conv}(w, \{e_{i_1 \dots i_d}\}_{(i_1, \dots, i_d) \in I}) = \{\eta w + \sum_{j=1}^d \sum_{i \in I_j} \alpha_{ij} e_i^j \mid (\alpha_{ij}, \eta) \in A_I\}$. Note the latter set can be parametrized by $\sum_{j=1}^d |I_j| + 1$ variables and hence should be easier to optimize over. One strategy is to use bisection to choose η by optimizing over α for each fixed η . Jointly optimizing η and α might be hard as projection to A_I is not easily computable.

An alternative parametrization introduces a slightly larger convex set. Indeed, consider $B_{w,I} = \{(\alpha_{ij}, \eta_j)_{1 \leq j \leq d, i \in I_j} \mid \alpha_{ij} \geq 0 \forall i, j, \eta_j \geq 0 \forall j, \sum_{i \in I_j} \alpha_{ij} + \eta_j \sum_{i \notin I_j} [w]_i^j = 1\}$. Then

$$\mathbf{conv}(w, \{e_{i_1 \dots i_d}\}_{(i_1, \dots, i_d) \in I}) \subset \left\{ \sum_{j=1}^d \left(\sum_{i \notin I_j} \eta_j [w]_i^j e_i^j + \sum_{i \in I_j} \alpha_{ij} e_i^j \right) \mid (\alpha_{ij}, \eta) \in B_{w,I} \right\}.$$

Note the latter set has $\sum_{j=1}^d |I_j| + d$ variables instead of $\sum_{j=1}^d |I_j| + 1$ variables as in the previous approach. However, note that optimizing over variables in $B_{w,I}$ is actually easier as $B_{w,I}$ is a product of scaled simplices which enables faster projection.

Algorithm 1 Frank-Wolfe with line search

Input: initialization $x_0 \in \mathbf{E}$
for $t = 1, 2, \dots$, **do**
 Linear optimization oracle (LOO): Compute $v_t \in \arg \min_{v \in \mathbf{E}} \langle v, \nabla f(x) \rangle$.
 Line search: solve $\hat{\eta} = \arg \min_{\eta \in [0,1]} f(\eta x_t + (1 - \eta)v_t)$ and set $x_{t+1} = \hat{\eta} x_t + (1 - \hat{\eta})v_t$.
end for

Algorithm 2 k FW for polytope

Input: initialization $x_0 \in \Omega$, and an integer $k > 0$
for $t = 1, 2, \dots$, **do**
 k linear optimization oracle (k LOO): compute k extreme points, v_1, \dots, v_k with smallest $\langle v, \nabla f(x_t) \rangle$ among all extreme points of $v \in \Omega$.
 k direction search (k DS): Solve $\min_{x \in \mathbf{conv}(v_1, \dots, v_k, x_t)} f(x)$ to obtain x_{t+1} .
end for

Algorithm 3 k FW for other Ω

Same as Algorithm 2, replacing the k LOO (with input $\nabla f(x_t)$) and k DS (with input consisting of x_t and the output of k LOO, and output $x_{t+1} = x_{k\text{DS}}$), as described in Section 2.2.

2.2 Stronger subproblem oracle for nonpolytope Ω

In this section, we explain how to extend k FW to operate on the unit group norm ball, spectrahedron, and nuclear norm ball. We shall *redefine* the k LOO and k DS accordingly.

2.2.1 Group norm ball

Let us first define the group norm ball. Given a partition $\mathcal{G} = \{g_1, \dots, g_l\}$ of the set $[n] = \{1, \dots, n\}$ ($\cup_{g \in \mathcal{G}} g = [n]$ and $g_i \cap g_j = \emptyset$ for $i \neq j$), the group norm and the unit group norm ball are

$$\|x\|_{\mathcal{G}} := \sum_{g \in \mathcal{G}} \|x_g\|, \quad \forall x \in \mathbb{R}^n \quad \text{and} \quad \mathbf{B}_{\|\cdot\|_{\mathcal{G}}} = \{x \in \mathbb{R}^n \mid \|x\|_{\mathcal{G}} \leq 1\}, \quad \text{respectively.} \quad (4)$$

Here the base norm $\|\cdot\|$ can be any ℓ_p norm, or even some matrix norms. We restrict our attention to the ℓ_2 norm in the main text for ease of presentation⁶. The vector x_g is formed by the entries of x with indices in g .

Let us now define k LOO and k DS for the group norm ball $\mathbf{B}_{\|\cdot\|_{\mathcal{G}}}$.

k LOO. Given an input $y \in \mathbb{R}^n$, k LOO outputs the k groups $v_1, \dots, v_k \in \mathcal{G}$ with largest $\|y_v\|$ among all $v \in \mathcal{G}$. Here the k best “directions” are not vectors, but groups. Notice the groups $g \in \mathcal{G}$ are disjoint, so $\sum_{i=1}^k \|y_{v_i}\| \leq \|y\|_{\mathcal{G}}$. In this sense, k LOO for the group norm ball generalizes k LOO for the simplex.

k DS. Given inputs $w \in \mathbf{B}_{\|\cdot\|_{\mathcal{G}}}$ and $v_1, \dots, v_k \in \mathcal{G}$, k DS for the group norm ball optimizes the objective $f(x)$ over convex combinations of w and vectors supported on $\cup_{i=1}^k v_i$. To parametrize vectors supported on $\cup_{i=1}^k v_i$, we introduce a variable $\lambda^{v_1, \dots, v_k} \in \mathbb{R}^n$ supported on $\cup_{i=1}^k v_i$. That is, $\lambda_i^{v_1, \dots, v_k} = 0$ for all $i \notin \cup_{i=1}^k v_i$. Our decision variable x is written as

$$x = \eta w + \lambda^{v_1, \dots, v_k}, \quad \text{where} \quad \eta + \|\lambda^{v_1, \dots, v_k}\|_{\mathcal{G}} \leq 1, \quad \eta \geq 0. \quad (5)$$

We solve the following problem to obtain $x_{k\text{DS}}$:

$$\text{minimize} \quad f(\eta w + \lambda^{v_1, \dots, v_k}) \quad \text{subject to} \quad \eta + \|\lambda^{v_1, \dots, v_k}\|_{\mathcal{G}} \leq 1, \quad \eta \geq 0. \quad (6)$$

We can again employ APG to solve this problem, as the projection step only requires $\mathcal{O}(k \log k + \sum_{i=1}^k |v_k|)$ time. (See more details in Section A.4.)

2.2.2 Nuclear norm ball

We now define k LOO and k DS for the unit nuclear norm ball $\mathbf{B}_{\|\cdot\|_{\text{nuc}}} = \{X \in \mathbb{R}^{n_1 \times n_2} \mid \|X\|_{\text{nuc}} \leq 1\}$, where $\|X\|_{\text{nuc}} = \sum_{i=1}^{\min(n_1, n_2)} \sigma_i(X)$, the sum of singular values.

k LOO. Given an input matrix $Y \in \mathbb{R}^{n_1 \times n_2}$, define the k best directions of the linearized objective $\min_{V \in \Omega(\alpha)} \langle V, Y \rangle$ to be the pairs $(u_1, v_1), \dots, (u_k, v_k)$, the top k left and right orthonormal singular vectors of Y . Collect the output as $U = [u_1, \dots, u_k] \in \mathbb{R}^{n_1 \times k}$ and $V = [v_1, \dots, v_k] \in \mathbb{R}^{n_2 \times k}$.

⁶See Section A.5 in the appendix for further discussion.

***k*DS.** Take as inputs $W \in \mathbf{B}_{\|\cdot\|_{\text{nuc}}}$ and $(U, V) \in \mathbb{R}^{n_1 \times k} \times \mathbb{R}^{n_2 \times k}$ with orthonormal columns. Inspired by [HR00], we consider the spectral convex combinations of W and $u_i v_i^\top$ instead of just convex combination:

$$X = \eta W + USV^\top \quad \text{where } \eta \geq 0, \eta + \|S\|_{\text{nuc}} \leq 1.$$

Next, we minimize the objective $f(X)$ parametrized by $(\eta, S) \in \mathbb{R}^{1+k^2}$ to obtain $X_{k\text{DS}}$:

$$\text{minimize } f(\eta W + USV^\top) \quad \text{subject to } \eta + \|S\|_{\text{nuc}} \leq 1, \eta \geq 0.$$

Again, we use APG to solve this problem. Projection requires singular value decomposition of a k^2 matrix, which is tolerable for small k . (See Section A.6 for details.)

A summary of $k\text{LOO}$ and $k\text{DS}$ for these sets appears in Table 6 and 7 in the appendix respectively. The case of spectrahedron has been addressed very recently by [DFXY20]. We give a self-contained description of its $k\text{LOO}$ and $k\text{DS}$ in Section A.1. The $k\text{FW}$ algorithm for unit group norm ball, spectrahedron, and unit nuclear norm ball is presented as Algorithm 3.

Remark 2. (Choice of k) Having discussed $k\text{FW}$ for various constraint sets, here we discuss the choice of k . Determining the choice of k is of great importance as our guarantees require k to be larger or equal to the underlying sparsity measure to observe significant speedup, see Definition 3 and results in Section 3. Domain knowledge is then particular helpful in this regard. In our experiments, for synthetic datasets, we have set k to be the ground truth of the sparsity measure. On real data, we determine k according to the expected sparsity level of the data (e.g. the expected number of support vectors in SVM, see Section 4 for details.)

Here we provide a adaptive method to adjust k , which is shown in Algorithm 4. The main idea is to increase k in every iteration until it cannot improve the relative decrease of the objective function. We found that setting the increasing factor $\varsigma = 2$ works every well in practice. For example, Figure 2 shows the results of $k\text{FW}$ with adaptive k on the Lasso problem. We see that the algorithm is able to find a (possibly) optimal k effectively with different initialization k_0 . We also found similar performance (not shown here) in the experiments of other tasks discussed in Section 4.

Algorithm 4 $k\text{FW}$ with adaptive k

Input: initialization x_0 and k_0 , parameter $\varsigma > 1$, $inc = \text{True}$
for $t = 0, 1, \dots$, **do**
 Compute $f(x_t)$
 if $t = 2$ **then**
 $k_t = \varsigma k_{t-1}$
 end if
 if $t > 2$ and $inc = \text{True}$ **then**
 if $(f(x_{t-1}) - f(x_t))/f(x_{t-1}) > (f(x_{t-2}) - f(x_{t-1}))/f(x_{t-2})$ **then**
 $k_t = \varsigma k_{t-1}$
 else
 $inc = \text{False}$
 end if
 end if
 $k\text{LOO}$ step
 $k\text{DS}$ step
end for

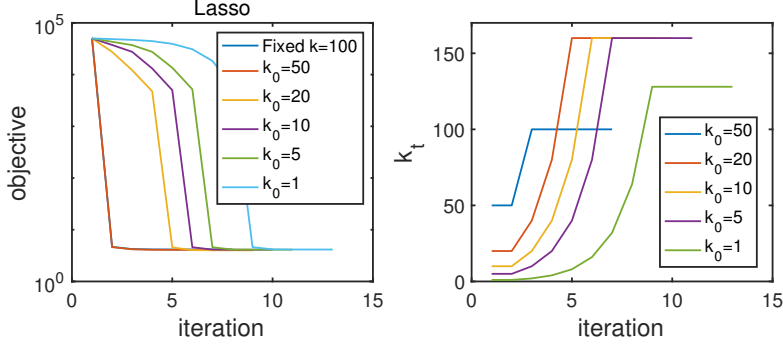


Figure 2: k FW with adaptive k (Algorithm 4) for Lasso

3 Theoretical guarantees

In this section, we first present a few definitions and conditions required to state our results. Then we present the theorems and provide intuitions. Proofs are deferred to Section B.4 and B.5.

3.1 Analytical conditions

Here we define the sparsity measure r_* for each constraint set Ω and the complementarity measure δ .

Definition 3 (Sparsity measure r_*). *Suppose the solution x_* of (1) is unique.*

- Polytope: *The sparsity measure r_* is the number of extreme points of the smallest face $\mathcal{F}(x_*)$ of Ω containing x_* .*
- Group norm ball: *The sparsity measure r_* is the number of groups $g \in \mathcal{G}$ such that $(x_*)_g \neq 0$, or equivalently, the cardinality of the set $\mathcal{F}(x_*) := \{g \mid (x_*)_g \neq 0\}$:*
- Spectrahedron and unit nuclear norm ball: *The sparsity measure r_* is $\text{rank}(X_*)$, or equivalently, the dimension of $\mathcal{F}(X_*) = \text{range}(X_*)$.*

In short, the sparsity is the cardinality or the dimension of the support set $\mathcal{F}(x_*)$.

Definition 4 (Strict complementarity). *Problem (1) admits strict complementarity if it has a unique solution $x_* \in \partial\Omega$ and $-\nabla f(x_*) \in \text{relint}(N_\Omega(x_*))$ ⁷ The complementarity measure δ is the gap between the inner products of x_* and the elements of the complementary set $\mathcal{F}^c(x_*)$ defined below:*

$$\delta = \min\{\langle u, \nabla f(x_*) \rangle - \langle x_*, \nabla f(x_*) \rangle \mid u \in \mathcal{F}^c(x_*) \subseteq \Omega\}. \quad (7)$$

The complementary set $\mathcal{F}^c(x_*)$. Morally, the complementary set $\mathcal{F}^c(x_*)$ is the complement (in Ω) of elements supported in $\mathcal{F}(x_*)$. Our formal definition also respects the vector structure of these sets.

- Polytope: *The complementary space $\mathcal{F}^c(x_*)$ is the convex hull of all vertices not in $\mathcal{F}(x_*)$.*
- Group norm ball: *The complementary space $\mathcal{F}^c(x_*)$ is the set of all vectors in Ω not supported in $\mathcal{F}(x_*) = \{g \mid (x_*)_g \neq 0\}$.*
- spectrahedron and nuclear norm ball: *The complementary space $\mathcal{F}^c(X_*)$ is the set of all matrices in Ω with column space orthogonal to $\mathcal{F}(X_*) = \text{range}(X_*)$.*

⁷Here $\partial\Omega$ is the topological boundary of Ω under the standard topology of \mathbf{E} . The set $N_\Omega(x_*)$ is the normal cone of Ω at x_* , i.e. $N_\Omega(x_*) = \{y \mid \langle y, x \rangle \leq \langle y, x_* \rangle, \forall x \in \Omega\}$, and $\text{relint}(\cdot)$ is the relative interior.

Table 8 in the appendix catalogues r_* , $\mathcal{F}(x_*)$, \mathcal{F}^c , and δ for several sets Ω . Note that the definition of the gap δ is always nonnegative due to optimality condition of (1). It is indeed positive when strict complementarity holds as shown in Lemma 11 in the appendix.

Remarks on strict complementarity. Two aspects of strict complementarity have important implications for k FW. (See further discussion in B.1.) First, structurally, the strict complementarity condition ensures robustness of r_* under perturbations of the problem. Indeed, consider the problem

$$\min_{x \in \Delta^n} \|x - \sigma e_1\|^2 + \langle c, x \rangle. \quad (8)$$

For $c = 0$ and any $\sigma \in [0, 1]$, the unique solution $x_* = \sigma e_1$, which is also sparse. However, it can be easily verified that strict complementarity *fails* in this case. As a result, almost any small perturbation $c \neq 0$ results in a solution with sparsity $r_* > 1$. We refer the reader to Example B.1 in the appendix and to [Gar20, Table 2], and to [Gar19a, Lemma 2 and 10] for more discussion on the relationship between complementarity and robustness of the solution sparsity.

Second, algorithmically, the proof of Theorem 7 and 10 reveal that k FW identifies the support set $\mathcal{F}(x_*)$ once the iterate is near x_* . The gap δ tells us how close it must be to identify the support.

We introduce the quadratic growth condition, a strictly weaker version of strong convexity. It has been studied in [DL18, NNG19] to ensure linear convergence of some first order algorithms, and is also necessary as shown in [NNG19].

Definition 5 (Quadratic growth). *Problem (1) admits quadratic growth with parameter $\gamma > 0$ if it has a unique solution x_* and for all $x \in \Omega$, $f(x) - f(x_*) \geq \gamma \|x - x_*\|^2$.*

Remarks on quadratic growth. For all constraint set Ω considered in this paper, quadratic growth holds under strict complementarity for strongly convex g in (1), $\min_{x \in \Omega} g(\mathcal{A}x) + \langle c, x \rangle$. (See Theorem 12 in the appendix for a proof.) Quadratic growth also holds for almost all c if g and Ω are semi-algebraic [DIL16, Corollary 4.8].

3.2 Guarantees for k FW

Our first theorem states that k FW never requires more iterations than FW.

Theorem 6. *Suppose f is L_f -smooth and convex and Ω is convex compact with diameter D . Then for any $k \geq 1$ and for all $t \geq 1$, the iterate x_t in k FW (Algorithm 2 and 3) satisfies*

$$f(x_t) - f(x_*) \leq \frac{L_f D^2}{t}. \quad (9)$$

Proof. The inequality (9) follows from the proof of convergence of FW as in [Jag13] by noting that the vector $v_t = \arg \min_{v \in \Omega} \langle \nabla f(x_t), v \rangle$ is feasible for the k DS minimization problem. \square

The theorem shows that k FW converges faster when $k \geq r_*$ for the polytope and group norm ball.

Theorem 7. *Suppose that f is L_f -smooth and convex, Ω is convex compact with diameter D , Problem (1) satisfies strict complementarity and quadratic growth, and $k \geq r_*$. If the constraint set Ω is a polytope or a unit group norm ball, then the gap $\delta > 0$ and k FW finds x_* in at most $T + 1$ iterations, where T is*

$$T = \frac{4L_f^3 D^4}{\gamma \delta^2}. \quad (10)$$

Proof. The proof follows from the intuition that once x_t is close to x_* , the set $\mathcal{F}(x_*)$ can be identified using $\nabla f(x_t)$. The fact that $\delta > 0$ is shown in Lemma 11. Let us now consider Algorithm 2 whose constraint set Ω is a polytope. Using quadratic growth in the following step (a), and Theorem 6 in the following second step (b), and the choice in the following step (c), the iterate x_t with $t \geq T$ satisfies that

$$\|x_t - x_*\| \stackrel{(a)}{\leq} \sqrt{\frac{1}{\gamma}(f(x_t) - f(x_*))} \stackrel{(b)}{\leq} \sqrt{\frac{L_f D^2}{\gamma T}} \stackrel{(c)}{\leq} \frac{\delta}{2L_f D}. \quad (11)$$

Next, for any $t \geq T$, we have that for any vertex v in $\mathcal{F}(x_*)$, and any vertices u in $\mathcal{F}^c(x_*)$,

$$\begin{aligned} \langle \nabla f(x_t), v \rangle - \langle \nabla f(x_t), u \rangle &= \langle \nabla f(x_*), v - u \rangle + \langle \nabla f(x_t) - \nabla f(x_*), v - u \rangle \\ &\stackrel{(a)}{\leq} -\delta + \langle \nabla f(x_t) - \nabla f(x_*), v - u \rangle \stackrel{(b)}{\leq} -\frac{\delta}{2}. \end{aligned} \quad (12)$$

Here in step (a), we use the definition of δ in (7) and $\langle x_*, \nabla f(x_*) \rangle = \langle v, \nabla f(x_*) \rangle$ using the optimality condition for Problem (1) and $\mathcal{F}(x_*)$ being the smallest face containing x_* . In step (b), we use the bound in (11), Lipschitz continuity of $\nabla f(x)$, and $\|v - u\| \leq D$.

Thus, the k LOO step will produce all the vertices in $\mathcal{F}(x_*)$ as $k \geq r_*$ after $t \geq T$, and so x_* is a feasible and optimal solution of the optimization problem in the k direction search step. Hence, Algorithm 2 finds the optimal solution x_* within $T + 1$ many steps. The case for unit group norm ball can be similarly analyzed and we defer the detail to Section B.4 in the appendix. \square

Remark 8 (The burn-in period T). The initial “burn-in” period scales as $\mathcal{O}\left(\frac{4L_f^3 D^4}{\gamma \delta^2}\right)$, which is arguably too large for certain choice of L_f, D, γ , and δ . It is possible to remedy the situation for many polytopes by incorporating the technique from [GM16] by simply adding the atom $\gamma_t(v_t^+ - v_t^-)$ proposed in [GM16, Algorithm 3] into our k DS. Utilizing their convergence rate result [GM16, Theorem 1], the time T can be improved to $\frac{\text{card}(x_*)2L_f D^2}{\gamma} \log\left(\frac{4L_f^2 D^2}{\delta^2 \gamma}\right)$, where $\text{card}(x_*)$ is the number of nonzeros in x_* . However, we note that in our experiments, the number of iterations of k FW is extremely low and the estimate T is too pessimistic.

Remark 9 (Subproblem complexity). The finite complexity result for the polytope and group norm ball requires that each k DS solves the subproblem (3) exactly. A closer look reveals that the proof basically assumes that k FW achieves the worst case rate $\mathcal{O}(1/t)$ rate in the beginning, and once the iterate is close to x_* , k LOO finds the optimal face and k DS finds the solution x_* . For a theoretical analysis purpose of lowering the complexity in terms of gradient computation, LOO, and k LOO, one can modify the algorithm (assuming knowing the constant L_f, D, γ, δ) so it first perform T many iterations of FW with stepsize rule $\mathcal{O}(1/t)$; and then perform one k LOO and one k DS. This algorithm will require T many gradient computation in the first stage and k many LOOs, and one k LOO and one k DS in the second stage. If APG is employed in solving the problem in k DS, one requires $\mathcal{O}\left(\frac{1}{\sqrt{\epsilon}}\right)$ gradient computation. In our experiments, we found the subproblem is not too hard to solve to high accuracy and employing k DS in the beginning significantly reduces the total time.

Convergence for the spectrahedron and nuclear norm ball differs because any neighborhood of X_* contains infinitely many matrices with rank $\leq r_*$. The proof appears in Section B.5 in the appendix.

Theorem 10. *Instate the assumption of Theorem 7. Then if the constraint set is the spectrahedron or the unit nuclear norm ball, the gap $\delta > 0$ and k FW satisfies that for any $t \geq T := \frac{72L_f^3}{\gamma\delta^2}$,*

$$f(X_{t+1}) - f(X_\star) \leq \left(1 - \min\left\{\frac{\gamma}{4L_f}, \frac{\delta}{12L_f}\right\}\right) (f(X_t) - f(X_\star)). \quad (13)$$

3.3 A limitation of k FW for polytopes and potential fixes

As stated in Theorem 7, k FW needs the parameter k to be greater than or equal to the sparsity level r_\star , which is the number of vertices of the optimal face instead of $1 + \dim(\mathcal{F}(x_\star))$, the face dimension plus one. The number r_\star can be arbitrarily larger than the dimension $1 + \dim(\mathcal{F}(x_\star))$ for some sets Ω . This in turn means that k has to be very large, at least in theory.

Indeed, the following Example 3.1 shows that if k is only larger than $1 + \dim(\mathcal{F}(x_\star))$, but not larger than r_\star , k FW can behave as bad as standard Frank-Wolfe. The slowdown occurs for the same reason as the zigzagging slowdown in Frank Wolfe: if all the vertices selected are nearly linearly dependent, they do not necessarily span the whole face, so x_\star may lie far from their convex hull even though they lie on the same face as x_\star .

Example 3.1 (A worst case example). Consider the following problem:

$$\begin{aligned} &\text{minimize} && f(x, y, z) := x^2 + y^2 + z \\ &\text{subject to} && x \in \Omega := \{(x, y, z) \mid \sqrt{x^2 + y^2} \leq 1 - z\}. \end{aligned} \quad (14)$$

The constraint set Ω is an ice-cream cone. It is easily verified that the origin $(0, 0, 0)$ is the solution and that strict complementarity holds for this problem. Now, if we start at $x^0 = (x_0, y_0, z_0) = (0, 0, 0.1)$ and use FW to solve the problem, it can be shown that FW will produce iterates $x^1, x^2, x^3, \dots, x^t, \dots$ that converge to the solution $(0, 0, 0)$ with rate $f(x^t) \geq \frac{c}{t}$ for some constant c . A numerical demonstration of the slow convergence is shown by the line “FWSOC” in Figure 5 for the objective value of the first 30 iterations.

Next consider the constraint set $\Omega_n = \mathbf{conv}((0, 0, 1), \{\theta_i\}_{i=1}^n)$ where $\theta_i = (\cos(2\pi i/n), \sin(2\pi i/n), 0)$. In other words, Ω_n is the polytope being a convex hull of the vertex $(0, 0, 1)$ and a n -polygon on the x - y plane. We now consider

$$\begin{aligned} &\text{minimize} && f(x, y, z) := x^2 + y^2 + z \\ &\text{subject to} && x \in \Omega_n. \end{aligned} \quad (15)$$

The n -polygon on the x - y plane approximates the unit disk for large n , also see Figure 4 for an illustration of this approximation. Hence, the feasible region Ω_n approximates Ω for large n (see 3 for a comparison), and we expect FW applied to Problem (14) and (15) behaves similarly. One can verify that the origin is still the solution and that strict complementarity continues to hold for $n \geq 3$. Moreover, the strict complementarity parameter δ_n for this problem is exactly the same for all $n \geq 3$. The quadratic growth parameter γ also stabilizes for all large n . Now consider running k FW starting from $x^0 = (x_0, y_0, z_0) = (0, 0, 0.1)$. Then for any T and k , there is an N such that for all $n > N$, the k FW iterate $x^{t, k\text{FW}}$ does not stop after T iterations and $f(x^{t, k\text{FW}}) \geq \frac{c}{2t}$ for all $t \leq T$. This is because for each T and k , we can increase n so that Ω_n is close enough to Ω . The closeness in the feasible region make the vertices found by k FW tend to be quite close to each other (just like the vertices found by FW), and they fail to form a convex combination of the optimal solution. Hence $x^{t, k\text{FW}}$ will be very close to x^t and by our result from previous paragraph, we should have $f(x^{t, k\text{FW}}) \geq \frac{c}{2t}$ for all $t \leq T$. A numerical illustration of this fact for the first 30 iterations of FW and k FW can be found in Figure 5. In this case, the dimension of the optimal face is always 2, but the number of vertices on the optimal face, r_\star , grows with n and can be arbitrarily larger than 2.

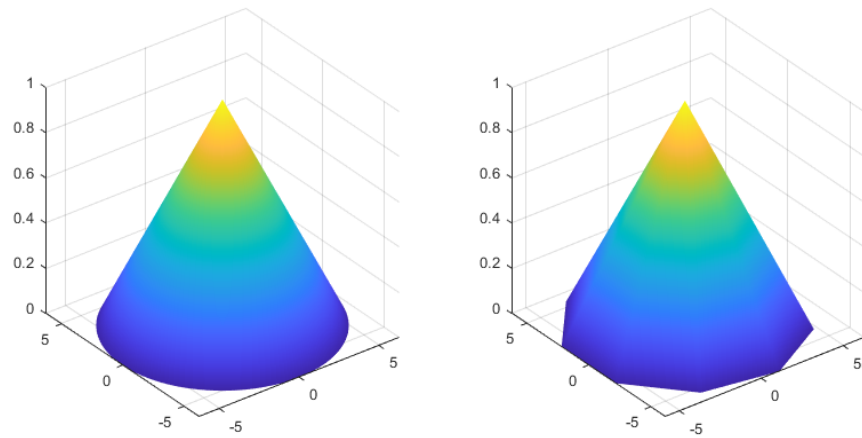


Figure 3: The left plot shows a second order cone in (14) . The right plot shows a polyhedron in (15) that approximates the second order cone.

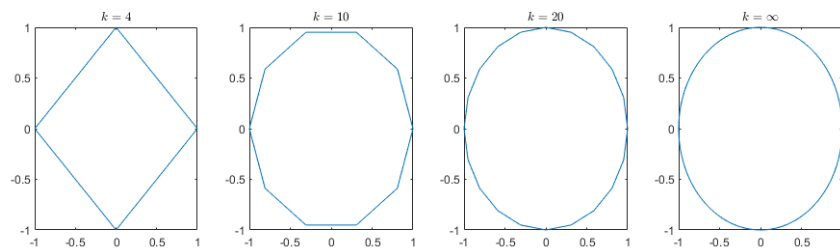


Figure 4: From left to right, we show the n -polygon, the bottom of the feasible region (15), that approximates the disk, the bottom of the second order cone.

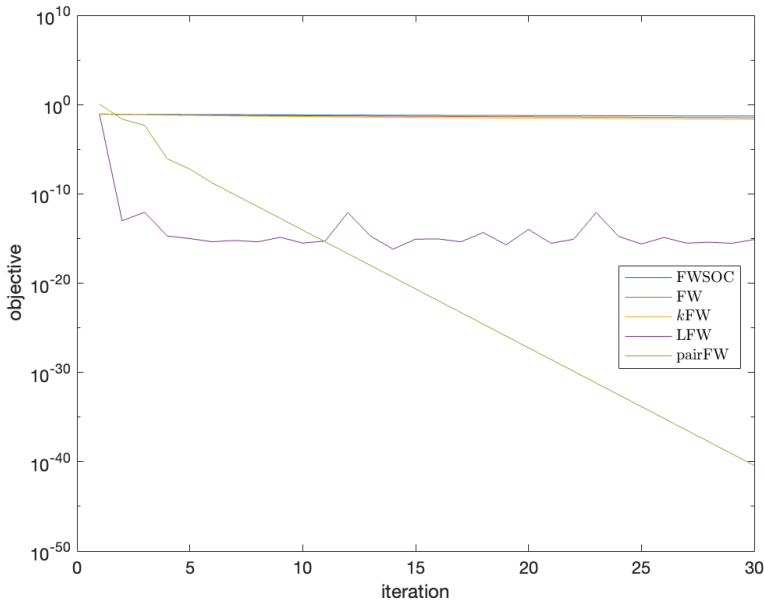


Figure 5: The objective value of different algorithms for (14) and (15). FWSOC shows the behavior of FW applied to (14). The other lines are different algorithms applies to (15). LFW stands for limited memory Frank-Wolfe, which always keep the most recent 2 vertices found by LOO, and optimal over the convex hull of the current iterate and these two past vertices. PairFW stands for pairwise FW.

A quick fix We could remedy the problem with a stronger oracle: for example, one that outputs vertices that are always linear independent, or (even better) an oracle that can output a set of vertices whose convex hull contains x_* whenever the iterate is close to x_* . If the oracle can achieve this latter property, then $k = 1 + \dim(\mathcal{F}(x_*))$ suffices for fast convergence by Caratheodory’s theorem. Hence we avoid the dependence on r_* defined here. These strong oracles exist for some sets, such as the simplex, the ℓ_1 norm ball, and the spanning tree in a graph (in the sense of orthogonality), but in general they may be prohibitively expensive to compute.

The relation between r_* and $\dim(\mathcal{F}(x_*))$ For polytopes encountered in practice, the relation between r_* and the face dimension varies. For the probability simplex and the ℓ_1 norm ball, $r_* = 1 + \dim(\mathcal{F}(x_*))$. Frank Wolfe is often used to optimize over these sets, and our algorithm presents a substantial advantage here. For other types of polytope, the dependence of r_* on the face dimension can be polynomial or exponential, e.g., products of simplices and Birkhoff polytopes.

Our responses to the limitation The limitation of $k \geq r_*$ instead of $k \geq \dim(\mathcal{F}(x_*)) + 1$ of our theory need not spell disaster in practice: small k can still work. First, if x_* is a vertex or x_* lies on a 1 dimensional line segment, then $r_* = 2$ suffices. More generally, if x_* lies on a face with dimension independent of the ambient dimension n , then r_* is independent of n even if it is exponential in $\dim(\mathcal{F}(x_*))$. Second, even if r_* is polynomial or exponential in the dimension of the face $\mathcal{F}(x_*)$, it is sometimes still easy to solve the k LOO and k DS subproblem: for example, these subproblem are still easy for the simplex, a product of simplices, the ℓ_1 norm ball, or a product of ℓ_1 norm balls. See Remark 1 for a detailed discussion. Finally, as shown by the following example,

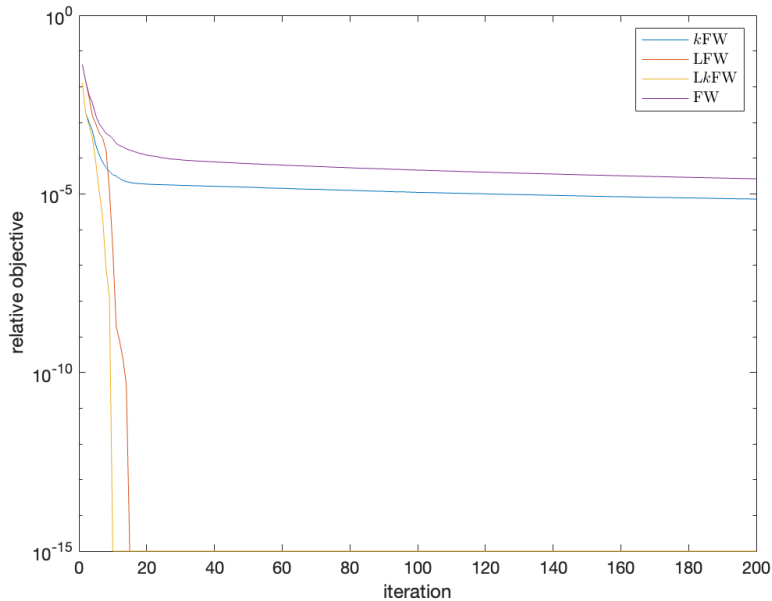


Figure 6: Relative objective $\frac{f(x)-f(x_*)}{f(x_*)}$ for the hypercube problem (16) of different algorithms.

we found that in numerics, a modified version of k FW which incorporates limited past information can limit the choice of k to $\mathcal{O}(\dim(\mathcal{F}(x_*)))$ even though the vanilla version may fail.

Example 3.2. We consider the problem of projection to the hypercube $[0, 1]^n$:

$$\begin{aligned} & \text{minimize} && f(x) := \|x - x_0\|_2^2 \\ & \text{subject to} && x \in [0, 1]^n. \end{aligned} \tag{16}$$

We perform experiments with $n = 50$ and set the first 10 coordinates of x_0 to be uniformly chosen from $[0, 1]$, and set the rest of the coordinates to be 2. This choice of x_0 ensures the strict complementarity condition is satisfied. We compute the optimal solution of (16) via Sedumi [Stu99] and found it has 40 ones and all the other entries are in $(0, 1)$. Note this face has 2^{10} many vertices though. Hence the optimal face is $\mathcal{F}(x_*)$ is 10 dimensional. We set $k = 10$ and we try (1) FW, (2) k FW with $k = 11$, (3) k FW with limited memory (LkFW), that is, we also keep the most recent $k - 1$ vertices found by LOO in the past $k - 1$ iterations, and then add them together with the output of k LOO into $2k - 1$ -DS. (4) FW with limited past information (LFW), which call LOO once in every iteration, but keep the most recent $k - 1$ vertices found by LOO in the past $k - 1$ iterations. The results of the objective value against the iteration is shown in Figure 6. It can be seen that once past information is incorporated, LkFW is able to find the optimal solution in very few iterations while the vanilla k FW behaves similarly to FW. It is also interesting LFW itself is as fast as LkFW for this problem.

4 Numerics

In this section, we perform experiments to see the empirical behavior of k FW. We first start with synthetic datasets, where we set k to be the ground truth of the sparsity measure. Next, we

experiment on real data, we determine k according to the expected sparsity level of the data (e.g. the expected number of support vectors in SVM).

4.1 Synthetic data

We compare our method k FW with FW, away-step FW (awayFW) [GM86], pairwise FW (pairFW)[LJJ15], DICG [GM16], and blockFW [AZHHL17] for the Lasso, support vector machine (SVM), group Lasso, and matrix completion problems on synthetic data. Details about experimental settings appear in the Appendix D. All algorithms terminate when the relative change of the objective is less than 10^{-6} or after 1000 iterations. As shown in Figure 7, k FW converges in many fewer iterations than other methods. Table 2 shows that k FW also converges faster in wall-clock time, with one exception (blockFW in matrix completion). Note that blockFW is sensitive to the step size while k FW has no step size to tune. More numerics can be found in Appendix D.

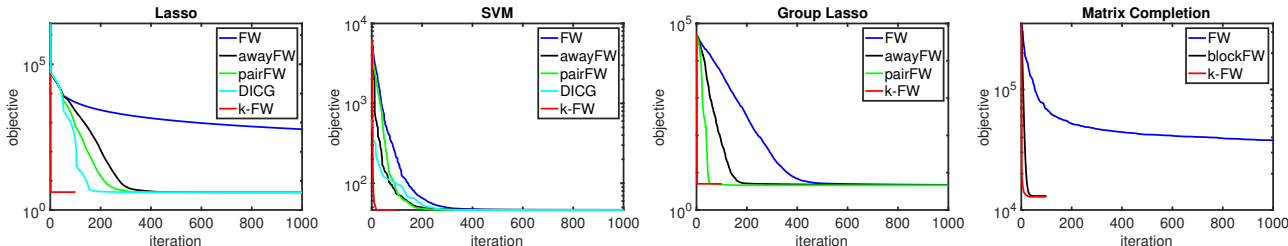


Figure 7: k FW vs. FW and its variants

Table 2: Computation time (seconds): the algorithms terminate when the relative change of the objective $< 10^{-6}$ or after 1000 iterations. The dash - means the algorithm is not suited to the problem.

	FW	awayFW	pairFW	DICG	blockFW	k FW
Lasso	>14	7	6	10	-	0.5
SVM	6	4.5	2.9	2.5	-	0.6
Group Lasso	17	6	1.8	-	-	0.3
Matrix completion	>180	-	-	-	1.8	4.8

Time of k LOO and k DS In the experiments, the time cost ratios k LOO: k DS are approximately: Lasso 0.6:1, SVM 0.03:1, Group Lasso 0.2:1, MC 0.1:1. The time of k FW spends on k DS occupies a major fraction of the total time. However, the spend is worthwhile as the number of iteration is extremely reduced indicated by our experiments.

4.2 Real data

First, we randomly choose 5000 samples of each digit of the MNIST [LBBH98] dataset to form a dictionary $A \in \mathbb{R}^{784 \times 50000}$. Given an image b from the rest of the dataset, we add Gaussian noise (zero mean and 0.1 variance) to it (denoted by \bar{b}) and use sparse coding to denoise, i.e. $\hat{x} = \operatorname{argmin}_x \|Ax - \bar{b}\|^2$ subject to $\|x\| \leq 2$. In k FW, we set $k = 50$. In every algorithm, the optimization is terminated if the relative change of the objective function is less than 10^{-4} or the iteration number reaches 500. The recovered image is $\hat{b} = A\hat{x}$. The recovery error is defined as $\operatorname{RE} = \|\hat{b} - b\|/\|b\|$. Table 3 shows three examples. We see that k FW is significantly faster than

other methods in all cases and the recovery error of k FW is much lower than DICG. Figure 8 shows some examples intuitively.

Table 3: Examples of denoising on MNIST (TC: time cost (second); RE: recovery error).

digit	metric	FW	awayFW	pairFW	DICG	k FW
0	TC	18.2	19.1	18.9	4.0	1.6
	RE	0.2634	0.2641	0.2645	0.2665	0.2639
1	TC	18.7	18.1	18.2	5.7	3.2
	RE	0.3725	0.3764	0.3731	0.4010	0.3632
2	TC	18.3	18.4	18.1	6.1	2.3
	RE	0.3272	0.3281	0.3267	0.3383	0.3258
3	TC	18.2	18.3	18.1	6.1	2.4
	RE	0.2577	0.2607	0.2587	0.2653	0.2581
4	TC	18.4	18.2	18.1	5.3	4.0
	RE	0.3240	0.3273	0.3263	0.3256	0.3249
5	TC	18.7	18.3	18.3	6.5	2.8
	RE	0.3136	0.3132	0.3134	0.3264	0.3110
6	TC	18.6	18.4	18.6	6.1	3.9
	RE	0.2772	0.2792	0.2800	0.2890	0.2772
7	TC	18.2	18.2	18.4	6.6	3.0
	RE	0.3315	0.3297	0.3301	0.3296	0.3237
8	TC	17.4	17.6	18.4	2.8	2.3
	RE	0.3072	0.3066	0.3072	0.3555	0.3069
9	TC	18.3	18.0	18.0	7.6	2.2
	RE	0.3575	0.3598	0.3573	0.3618	0.3535

Second, we consider the SVM classification task on the MNIST dataset. We randomly choose 5000 samples of digit “0” and 5000 samples of digit “6”. The training-testing ratio is 8:2. In k FW, we set $k = 50$. The time cost and classification accuracy (average of 10 trials) in the condition of different number of iterations are reported in Table 4. With 50 iterations, the SVM solved by k FW achieved a classification accuracy of 0.9934 while the accuracies of SVM solved by other algorithms are lower than 0.9. In general, the results in Table 4 indicate that k FW is much more efficient than other algorithms in solving the optimization of SVM.

Table 4: SVM (with second-order polynomial kernel, $C = 10$, and $\lambda = 0.1$) classification for digits “0” and “6” of MNIST (TC: time cost (second); Acc: classification accuracy).

iterations	metric	FW	awayFW	pairFW	DICG	k FW
10	TC	6.6	7.5	3.8	3.1	1.2
	Acc	0.5094	0.6514	0.5691	0.6650	0.8199
50	TC	44.0	48.6	19.6	14.9	5.6
	Acc	0.8331	0.8364	0.7997	0.8728	0.9934
200	TC	239.0	261.1	90.1	60.9	22.6
	Acc	0.9236	0.9852	0.9503	0.9915	0.9966
500	TC	722.3	743.5	265.1	155.4	55.7
	Acc	0.9834	0.9931	0.9916	0.9957	0.9962

Finally, we consider an inpainting problem for the gray-scale image shown in Figure 9. We

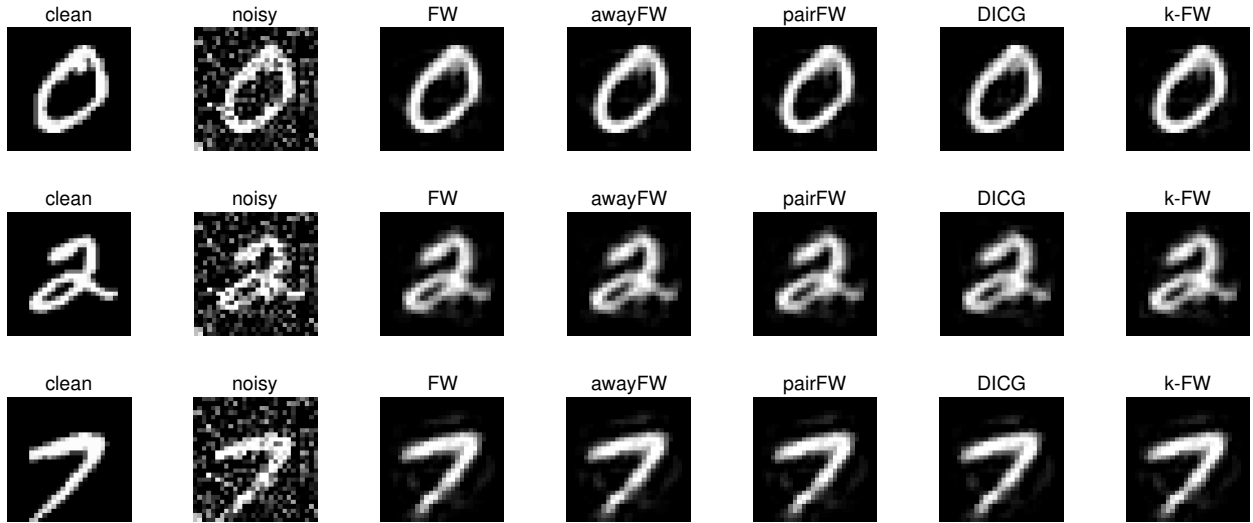


Figure 8

randomly remove 50% of the pixels. Since the image matrix X_{org} is approximately low-rank, we use $\|X\|_{\text{nuc}} \leq 0.8\alpha$, where α is the value of the nuclear norm of X_{org} . In blockFW and k FW, we set $k = 5$. In Figure 9, we see that blockFW with $\eta = 0.1$ outperformed our k FW slightly in terms of PSNR. In addition, the time cost of k FW is 2.5 times of blockFW. However, blockFW requires a well determined step size η .

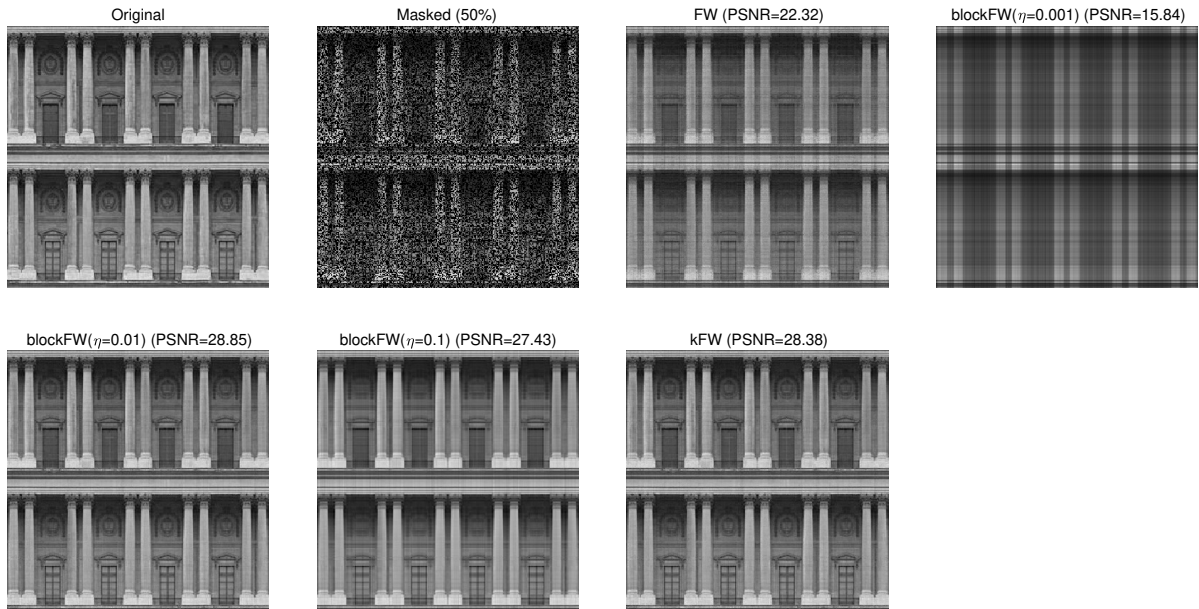


Figure 9: Image inpainting by matrix completion with different solvers.

5 Conclusion and discussion

This paper presented a new variant of FW, k FW, that takes advantage of sparse structure in problem solutions to offer much faster convergence than other variants of FW, both in theory and in practice. k FW avoids the Zigzag phenomenon by optimizing over a convex combination of the previous iterate and k extreme points of the constraint set, rather than one, at each iteration. The method relies on the ability to efficiently compute these k extreme points (k LOO) and to compute the update (k DS), which we demonstrate for a variety of interesting problems.

Apart from the algorithmic advance of the introduction of k LOO and k DS for various settings, theoretically, a more uniform, geometric definition of strict complementarity that unifies and extends previous work [DFXY20, Gar19a, Gar20], and allows us to handle a wide range of problems in a coherent framework.

Related work and comparison A recent line of work [DFXY20, Gar19a, Gar20, DCP20, CDLP21] utilizes the concept of strict complementarity or the local geometry of (1) near x_* to show faster convergence when the iterate is near the solution. [Gar19a] studies vanilla FW for spectrahedron with rank one solution and [DFXY20] shows how to deal with general rank by utilizing k LOO and k DS (specFW in their language). The work [Gar20] revisits away-FW and show the method achieves better local convergence rate. In [DCP20, CDLP21], the authors tries to accelerate away-FW when the iterate is close to the solution for polytope constraint.

Comparably, these past works are rather specific, in particular, strict complementarity is defined specific to each setting rather than in a uniform way. Nevertheless, the present work is inspired from [DFXY20] and the contribution of the present work is to distill and generalize the ideas there to various settings such as polytope, group norm ball, and nuclear norm ball. In particular, the extension to the nuclear norm from the spectrahedron is important for several reasons: (i) The nuclear norm ball (NNB) formulation is the natural problem form for rectangular matrix recovery problems; (ii) To apply the spectrahedron formulation to NNB formulation would require dilation, which doubles the number of variables. Moreover, a quadratic growth objective does not have quadratic growth after dilation, so existing theory for the spectrahedral case does not apply; (iii) Technically, our analysis is similar to [DFXY20] but introduces several novel elements; note in particular that the SC defined in the present paper generalizes that in [DFXY20].

The idea of utilizing multiple directions instead of just one is rooted in fully-corrective FW and related variants. It is also explored in recent works such as [AZHHL17, BRZ20]. [AZHHL17] deals with nuclear norm ball and computes multiple singular vectors in each iteration in order to make a gradient step. Note that even though [AZHHL17] considers computing k singular vectors, the k LOO is not based on the gradient but rather primal iterate - gradient, which may induces some computation difficulty due to the higher rank of iterates. More importantly, it may not converge for $k < r_*$ as shown in [AZHHL17, Figure 1], while k FW converges always as shown in Theorem 6. The work [BRZ20] considers how to identify the vertices on the optimal face via away-FW, however, the result is limited to probability simplex.

Future work We expect the core ideas that undergird k FW can be generalized to a wide variety of atomic sets in addition to those considered in this paper. We also expect the idea of k DS and a limited memory Frank-Wolfe, which uses most recent k points found by LOO, can still succeed for polytopes with r_* much larger than the dimension of the optimal face.

Acknowledgements

This work was supported in part by NSF Awards IIS-1943131 and CCF-1740822, the ONR Young Investigator Program, DARPA Award FA8750-17-2-0101, the Simons Institute, and Capital One. We would like to thank Billy Jin and Song Zhou for helpful discussions.

References

- [AZHHL17] Zeyuan Allen-Zhu, Elad Hazan, Wei Hu, and Yuanzhi Li. Linear convergence of a frank-wolfe type algorithm over trace-norm balls. In *Advances in Neural Information Processing Systems*, pages 6191–6200, 2017.
- [B⁺13] Francis Bach et al. Learning with submodular functions: A convex optimization perspective. *Foundations and Trends[®] in Machine Learning*, 6(2-3):145–373, 2013.
- [BBL99] Heinz H Bauschke, Jonathan M Borwein, and Wu Li. Strong conical hull intersection property, bounded linear regularity, jameson’s property (g), and error bounds in convex optimization. *Mathematical Programming*, 86(1):135–160, 1999.
- [BRZ20] Immanuel M Bomze, Francesco Rinaldi, and Damiano Zeffiro. Active set complexity of the away-step frank–wolfe algorithm. *SIAM Journal on Optimization*, 30(3):2470–2500, 2020.
- [BS17] Amir Beck and Shimrit Shtern. Linearly convergent away-step conditional gradient for non-strongly convex functions. *Mathematical Programming*, 164(1-2):1–27, 2017.
- [CDLP21] Alejandro Carderera, Jelena Diakonikolas, Cheuk Yin Lin, and Sebastian Pokutta. Parameter-free locally accelerated conditional gradients. *arXiv preprint arXiv:2102.06806*, 2021.
- [CDS01] Scott Shaobing Chen, David L Donoho, and Michael A Saunders. Atomic decomposition by basis pursuit. *SIAM review*, 43(1):129–159, 2001.
- [Cla10] Kenneth L Clarkson. Coresets, sparse greedy approximation, and the frank-wolfe algorithm. *ACM Transactions on Algorithms (TALG)*, 6(4):1–30, 2010.
- [CY11] Yunmei Chen and Xiaojing Ye. Projection onto a simplex. *arXiv preprint arXiv:1101.6081*, 2011.
- [DCP20] Jelena Diakonikolas, Alejandro Carderera, and Sebastian Pokutta. Locally accelerated conditional gradients. In *International Conference on Artificial Intelligence and Statistics*, pages 1737–1747. PMLR, 2020.
- [DFXY20] Lijun Ding, Yingjie Fei, Qiantong Xu, and Chengrun Yang. Spectral frank-wolfe algorithm: Strict complementarity and linear convergence. *arXiv preprint arXiv:2006.01719*, 2020.
- [DIL16] Dmitriy Drusvyatskiy, Alexander D Ioffe, and Adrian S Lewis. Generic minimizing behavior in semialgebraic optimization. *SIAM Journal on Optimization*, 26(1):513–534, 2016.

- [DL11] Dmitriy Drusvyatskiy and Adrian S Lewis. Generic nondegeneracy in convex optimization. *Proceedings of the American Mathematical Society*, pages 2519–2527, 2011.
- [DL18] Dmitriy Drusvyatskiy and Adrian S Lewis. Error bounds, quadratic growth, and linear convergence of proximal methods. *Mathematics of Operations Research*, 43(3):919–948, 2018.
- [DU18] Lijun Ding and Madeleine Udell. Frank-Wolfe style algorithms for large scale optimization. In *Large-Scale and Distributed Optimization*. Springer, 2018.
- [DU20] Lijun Ding and Madeleine Udell. On the regularity and conditioning of low rank semidefinite programs. *arXiv preprint arXiv:2002.10673*, 2020.
- [Epp90] David Eppstein. Finding the k smallest spanning trees. In *Scandinavian Workshop on Algorithm Theory*, pages 38–47. Springer, 1990.
- [Epp98] David Eppstein. Finding the k shortest paths. *SIAM Journal on computing*, 28(2):652–673, 1998.
- [Epp14] David Eppstein. k-best enumeration. *arXiv preprint arXiv:1412.5075*, 2014.
- [FGM17] Robert M Freund, Paul Grigas, and Rahul Mazumder. An extended frank-wolfe method with “in-face” directions, and its application to low-rank matrix completion. *SIAM Journal on optimization*, 27(1):319–346, 2017.
- [FW56] Marguerite Frank and Philip Wolfe. An algorithm for quadratic programming. *Naval research logistics quarterly*, 3(1-2):95–110, 1956.
- [Gar19a] Dan Garber. Linear convergence of frank-wolfe for rank-one matrix recovery without strong convexity. *arXiv preprint arXiv:1912.01467*, 2019.
- [Gar19b] Dan Garber. On the convergence of projected-gradient methods with low-rank projections for smooth convex minimization over trace-norm balls and related problems. *arXiv preprint arXiv:1902.01644*, 2019.
- [Gar20] Dan Garber. Revisiting frank-wolfe for polytopes: Strict complementarity and sparsity. *Advances in Neural Information Processing Systems*, 33:18883–18893, 2020.
- [GH15] Dan Garber and Elad Hazan. Faster rates for the frank-wolfe method over strongly-convex sets. In *32nd International Conference on Machine Learning, ICML 2015*, 2015.
- [GM86] Jacques Guélat and Patrice Marcotte. Some comments on wolfe’s ‘away step’. *Mathematical Programming*, 35(1):110–119, 1986.
- [GM16] Dan Garber and Ofer Meshi. Linear-memory and decomposition-invariant linearly convergent conditional gradient algorithm for structured polytopes. In *Advances in neural information processing systems*, pages 1001–1009, 2016.
- [GSB14] Tom Goldstein, Christoph Studer, and Richard Baraniuk. A field guide to forward-backward splitting with a FASTA implementation. *arXiv eprint*, abs/1411.3406, 2014.

- [GSB15] Tom Goldstein, Christoph Studer, and Richard Baraniuk. FASTA: A generalized implementation of forward-backward splitting, January 2015. <http://arxiv.org/abs/1501.04979>.
- [HQ85] Horst W Hamacher and Maurice Queyranne. K best solutions to combinatorial optimization problems. *Annals of Operations Research*, 4(1):123–143, 1985.
- [HR00] Christoph Helmberg and Franz Rendl. A spectral bundle method for semidefinite programming. *SIAM Journal on Optimization*, 10(3):673–696, 2000.
- [Jag13] Martin Jaggi. Revisiting frank-wolfe: Projection-free sparse convex optimization. In *Proceedings of the 30th international conference on machine learning*, number CONF, pages 427–435, 2013.
- [JS10] Martin Jaggi and Marek Sulovský. A simple algorithm for nuclear norm regularized problems. In *Proceedings of the 27th International Conference on International Conference on Machine Learning*, pages 471–478, 2010.
- [JTFF14] Armand Joulin, Kevin Tang, and Li Fei-Fei. Efficient image and video co-localization with frank-wolfe algorithm. In *European Conference on Computer Vision*, pages 253–268. Springer, 2014.
- [Law72] Eugene L Lawler. A procedure for computing the k best solutions to discrete optimization problems and its application to the shortest path problem. *Management science*, 18(7):401–405, 1972.
- [LBBH98] Yann LeCun, Léon Bottou, Yoshua Bengio, and Patrick Haffner. Gradient-based learning applied to document recognition. *Proceedings of the IEEE*, 86(11):2278–2324, 1998.
- [LJJ13] Simon Lacoste-Julien and Martin Jaggi. An affine invariant linear convergence analysis for frank-wolfe algorithms. *arXiv preprint arXiv:1312.7864*, 2013.
- [LJJ15] Simon Lacoste-Julien and Martin Jaggi. On the global linear convergence of frank-wolfe optimization variants. In *Advances in Neural Information Processing Systems*, pages 496–504, 2015.
- [LJJSP13] Simon Lacoste-Julien, Martin Jaggi, Mark Schmidt, and Patrick Pletscher. Block-coordinate frank-wolfe optimization for structural svms. In *International Conference on Machine Learning*, pages 53–61. PMLR, 2013.
- [LP66] Evgeny S Levitin and Boris T Polyak. Constrained minimization methods. *USSR Computational mathematics and mathematical physics*, 6(5):1–50, 1966.
- [MR01] Conrado Martínez and Salvador Roura. Optimal sampling strategies in quicksort and quickselect. *SIAM Journal on Computing*, 31(3):683–705, 2001.
- [Mur68] Katta G Murthy. An algorithm for ranking all the assignments in order of increasing costs. *Operations research*, 16(3):682–687, 1968.
- [NNG19] Ion Necoara, Yu Nesterov, and Francois Glineur. Linear convergence of first order methods for non-strongly convex optimization. *Mathematical Programming*, 175(1-2):69–107, 2019.

- [RFP10] Benjamin Recht, Maryam Fazel, and Pablo A Parrilo. Guaranteed minimum-rank solutions of linear matrix equations via nuclear norm minimization. *SIAM review*, 52(3):471–501, 2010.
- [Sra11] Suvrit Sra. Fast projections onto $\ell_{1,q}$ -norm balls for grouped feature selection. In *Joint European Conference on Machine Learning and Knowledge Discovery in Databases*, pages 305–317. Springer, 2011.
- [Stu99] Jos F Sturm. Using sedumi 1.02, a matlab toolbox for optimization over symmetric cones. *Optimization methods and software*, 11(1-4):625–653, 1999.
- [YL06] Ming Yuan and Yi Lin. Model selection and estimation in regression with grouped variables. *Journal of the Royal Statistical Society: Series B (Statistical Methodology)*, 68(1):49–67, 2006.
- [YUTC17] Alp Yurtsever, Madeleine Udell, Joel Tropp, and Volkan Cevher. Sketchy decisions: Convex low-rank matrix optimization with optimal storage. In *Artificial Intelligence and Statistics*, pages 1188–1196, 2017.
- [ZGU18] Song Zhou, Swati Gupta, and Madeleine Udell. Limited memory Kelley’s method converges for composite convex and submodular objectives. In *Advances in Neural Information Processing Systems*, pages 4414–4424, 2018.
- [ZS17] Zirui Zhou and Anthony Man-Cho So. A unified approach to error bounds for structured convex optimization problems. *Mathematical Programming*, 165(2):689–728, 2017.

A Table and Procedures for Section 2

A.1 k LOO and k DS for Spectrahedron

We define k LOO and k DS for the spectrahedron $\mathcal{SP}^n = \{X \in \mathbb{S}^n \mid X \succeq 0, \mathbf{tr}(X) = 1\}$ in this section.

k LOO. Given an input matrix $Y \in \mathbb{S}^n$, define the k best directions of the linearized objective $\min_{V \in \mathcal{SP}^n} \langle V, Y \rangle$ as the bottom k eigenvectors of Y , the eigenvectors corresponding to the k smallest eigenvalues. Call these vectors v_1, \dots, v_k and collect the output as $V = [v_1, \dots, v_k] \in \mathbb{R}^{n \times k}$.

k DS. Take as inputs $W \in \mathcal{SP}^n$ and $V = [v_1, \dots, v_k] \in \mathbb{R}^{n \times k}$ with orthonormal columns. Instead of convex combinations of W and $v_i v_i^\top$, we consider a spectral variant inspired by [HR00]:

$$X = \eta W + V S V^\top \quad \text{where} \quad \eta \geq 0, \quad S \in \mathbb{S}_+^k, \quad \eta + \mathbf{tr}(S) = 1.$$

We minimize the objective $f(X)$ over this constraint set to obtain the solution $X_{k\text{DS}}$ to k DS:

$$\text{minimize} \quad f(\eta W + V S V^\top) \quad \text{subject to} \quad \eta \geq 0, \quad S \in \mathbb{S}_+^k, \quad \text{and} \quad \eta + \mathbf{tr}(S) = 1.$$

Again, we use APG to solve this problem. Projection onto the constraint set requires eigenvalue decomposition (EVD) of a k^2 matrix, which is tolerable for small k . (See more detail in Section A.6)

A.2 k LOO of combinatorial optimization

In this section, we present Table 5 of the computational complexity of finding the k best solution for combinatorial optimizations. In our setting, the k best solution corresponds to the k best directions of k LOO. We then point out those k LOO that can be efficiently computed.

Let us first look at Table 5 for the complexity of LOO and k LOO.

Table 5: The time complexity of k LOO for different combinatorial problems. The matroid $M = (E, \mathcal{I})$ consists of the ground set E with n elements and the set of bases \mathcal{I} . The polytope is the convex hull of all bases in $[0, 1]^n$. The quantity α is the complexity of checking independence of a set. Here $r(M)$ is the rank of the matroid M . The $s - t$ cut is for a directed graph with n nodes, m edges, a source node s , and a sink node t . For each $s - t$ cut, a partition S, S^c of the vertex set with $s \in S$ and $t \in S^c$, we define its cut point as a vector in $[-1, 1]^m$ that has entry 1 for an edge from S to S^c , and an entry -1 for an edge from S^c to S . The $s - t$ cut polytope is the convex hull of all cut points in $[-1, 1]^m$. The path polytope considers all simple path from s to t for a directed acyclic graph with n nodes and m edges. The polytope is then the convex hull of all simple path point in $[0, 1]^m$. For an undirected graph with n nodes and m edges, the spanning tree polytope is the convex hull of all spanning tree in $[0, 1]^m$.

Polytope name	LOO complexity	k LOO complexity
Probability simplex	$\mathcal{O}(n)$	$\mathcal{O}(n + k)$ [MR01]
Polytope of bases of a matroid M	$\mathcal{O}(n \log n, n\alpha)$	$\mathcal{O}(n \log n + knr(M)\alpha)$ [HQ85]
The Birkhoff polytope	$\mathcal{O}(n^3)$	$\mathcal{O}(kn^3)$ [Mur68]
$s - t$ Cut Polytope (Directed Graph)	$\mathcal{O}(nm \log n)$	$\mathcal{O}(kn^4)$ [HQ85]
$s - t$ path Polytope(DAG)	$\mathcal{O}(m + n \log n)$	$\mathcal{O}(m + n \log n + kn)$ [Epp98]
Spanning tree Polytope	$\mathcal{O}(m + n \log n)$	$\mathcal{O}(m \log n + k \min(n, k)^{1/2})$ [Epp90]

Let us now list other polytopes with efficient k LOO with the assumption that $k \leq n$:

- The ℓ_1 norm ball $\{x \in \mathbb{R}^n \mid \sum_{i=1}^n |x_i| \leq \alpha\}$ admits a k LOO with time complexity $\mathcal{O}(n + k)$ by simply considering finding the k largest elements among $2n$ elements.
- The spanning tree polytope of an undirected graph $G(V, E)$ in $\mathbb{R}^{|E|}$ admits a k LOO with time complexity $\mathcal{O}(m \log n + k^2)$, where $m = |E|$ and $n = |V|$ [Epp90].
- The Birkhoff polytope, the convex hull of permutation matrices in $\mathbb{R}^{n \times n}$, admits a k LOO with time complexity $\mathcal{O}(kn^3)$ [Mur68]
- The path polytope of a directed acyclic graph $G(V, E)$ in $\mathbb{R}^{|E|}$ admits a k LOO with time complexity $\mathcal{O}(m + n \log n + k \min(n, k)^{1/2})$, where $m = |E|$ and $n = |V|$ [Epp98].

Optimization over the probability simplex is useful for fitting support vector machines [Cla10, Problem (24)]. The ℓ_1 norm ball plays a key role in sparse signal recovery [CDS01]. The path polytope appears in applications in video-image co-localization [JTFF14].

A.3 Examples of k LOO and k DS

This section presents Table 6, which presents examples of efficiently-computable k LOO, and 7, which presents examples of efficiently-computable k DS.

Table 6: k LOO examples: The input is a vector y for the polytope and unit group norm ball (with base norm ℓ_2 norm), and a matrix Y for the spectrahedron and unit nuclear norm ball.

Name	k best direction and output	k LOO cost
Polytope	k extreme points v_i s with k smallest $\langle v, y \rangle$ among all extreme points v	See Table 5
Unit group norm ball	k groups $v_1, \dots, v_k \in \mathcal{G}$ of the largest ℓ_2 norm of y	$\mathcal{O}((\sum_{i=1}^k v_i) + k \log k)$
Spectral simplex	bottom k eigenvector v_i s of Y , output $V = [v_1, \dots, v_k]$	Computing bottom k eigenvectors
Unit nuclear norm Ball	top k left, right singular vectors (u_i, v_i) of Y , output $U = [u_1, \dots, u_k]$, $V = [v_1, \dots, v_k]$.	Computing top k singular vectors

Table 7: k direction search examples. We present the parametrization of the vector x or matrix X in the second column. The k DS optimization problem is to minimize $f(x)$ or $f(X)$ over the parametrization. The input is a vector w or a matrix W in Ω and another of the form output by k LOO.

Name	Parametrization of x or X	Parameter variable	Parameter constraint (p.r.)	Main cost of proj to p.r.
Polytope	$\eta w + \sum_{i=1}^k \lambda_i v_i$	$(\eta, \lambda) \in \mathbb{R}^{k+1}$	$(\eta, \lambda) \in \Delta^{k+1}$	$\mathcal{O}(k \log(k))$
Unit Group norm ball	$\eta w + \lambda^{v_1, \dots, v_k}$	$(\eta, \lambda^{v_1, \dots, v_k}) \in \mathbb{R}^{1+n}$	$\eta + \ \lambda^{v_1, \dots, v_k}\ _{\mathcal{G}} \leq 1$	$\mathcal{O}(k \log(k)) + \mathcal{O}(\sum_{i=1}^k v_i)$
Spectrahedron	$\eta W + V S V^\top$	$(\eta, S) \in \mathbb{R} \times \mathbb{S}^k$	$\eta \geq 0, S \succeq 0$ $\eta + \text{tr}(S) = 1$	a full EVD of a k^2 matrix
Unit nuclear norm Ball	$\eta W + U S V^\top$	$(\eta, S) \in \mathbb{R}^{1+k^2}$	$\eta \geq 0, \eta + \ S\ _{\text{nuc}} \leq 1$	a full SVD of a k^2 matrix

A.4 Projection Step in APG for k DS of group norm ball

Here we described the projection procedure in k DS for group norm ball when the base norm is ℓ_2 norm. Suppose we want to solve the projection problem given $(\eta_0, \lambda_0^{v_1, \dots, v_k}) \in \mathbb{R}^{1+n}$ with decision variable η and $\lambda^{v_1, \dots, v_k}$:

$$\text{minimize } \|(\eta_0, \lambda_0^{v_1, \dots, v_k}) - (\eta, \lambda^{v_1, \dots, v_k})\|_2 \quad \text{subject to } \eta + \|\lambda^{v_1, \dots, v_k}\|_{\mathcal{G}} \leq 1, \eta \geq 0. \quad (17)$$

Here we further require that $\lambda_0^{v_1, \dots, v_k}$ and $\lambda^{v_1, \dots, v_k}$ are supported on $\cup_{i=1}^k v_i$. We denote the optimal solution as $\eta^*, (\lambda^{v_1, \dots, v_k})^*$.

Since $\lambda^{v_1, \dots, v_k}$ is only supported on $\cup_{i=1}^k v_i$, we can consider it as a vector in $\mathbb{R}^{v_1 + \dots + v_k}$ and $\|\lambda^{v_1, \dots, v_k}\|_{\mathcal{G}} = \sum_{i=1}^k \|\lambda_{v_i}^{v_1, \dots, v_k}\|_2$. The procedure for projection is as follows:

1. First compute the (η^*, a^*) that solves

$$\begin{aligned} & \text{minimize}_{(\eta, a)} \|(\eta, a) - (\eta_0, \llbracket \lambda_0^{v_1, \dots, v_k} \rrbracket_{v_i}^k)\|_2 \\ & \text{subject to } (\eta, a) \in \mathbb{R}_+^{k+1}, \quad \eta + \sum_{i=1}^k a_i \leq 1. \end{aligned} \quad (18)$$

Here \mathbb{R}_+^{k+1} is the nonnegative orthant in \mathbb{R}^{k+1} .

2. Next, for each v_i , we compute $(\lambda^{v_1, \dots, v_k})_{v_i}^*$ by solving

$$(\lambda^{v_1, \dots, v_k})_{v_i}^* = \arg \min_{\|\lambda_{v_i}^{v_1, \dots, v_k}\| \leq a_i^*} \|[\lambda_0^{v_1, \dots, v_k}]_{v_i} - \lambda_{v_i}^{v_1, \dots, v_k}\|_2.$$

The first step requires a projection to the convex hull of simplex and 0 and can be done in time $\mathcal{O}(k \log k)$. The second step requires projection to ℓ_2 norm ball which is a simple scaling. The correctness can be verified by decomposing each $\lambda_{v_i}^{v_1, \dots, v_k} = \alpha_i w_i$ where $\alpha_i \geq 0$ and w_i has ℓ_2 norm 1. For general ℓ_p norm, one has to find a root of a monotone function. This problem can be solved by bisection [Sra11].

A.5 Discussion on the norm of group norm ball

For the main Theorems 6, 7, and 10, the results holds for any arbitrary norm. The positive gap in Lemma 11 also holds for an arbitrary norm. However, the authors have not been able to verify whether strict complementarity implies quadratic growth for norms other than the ℓ_2 norm.

A.6 Projection Step in APG for k DS of spectrahedron, and nuclear norm ball

We consider how to compute the projection step of k DS for the spectrahedron and nuclear norm ball.

Spectrahedron We want to find (η^*, S^*) that solves

$$\text{minimize } \|(\eta, S) - (\eta_0, S_0)\|_2, \quad \text{subject to } S \in \mathbb{S}_+^k, \eta \geq 0, \text{tr}(S) + \eta = 1.$$

Here $\|(\eta, S)\|_2 = \sqrt{\eta^2 + \|S\|_F^2}$. The procedures are as follows:

1. Compute the eigenvalue decomposition of $S_0 = V\Lambda_0V^\top$, where $\Lambda_0 \in \mathbb{S}^k$ is a diagonal matrix with diagonal $\vec{\lambda}_0 = (\lambda_1, \dots, \lambda_k)$.
2. Compute $(\eta^*, \vec{\lambda}^*) = \arg \min_{(\eta, \vec{\lambda}) \in \Delta^{k+1}} \|(\eta_0, \vec{\lambda}_0) - (\eta, \vec{\lambda})\|_2$.
3. Form $S^* = V\text{diag}(\vec{\lambda}^*)V^\top$. Here $\text{diag}(\lambda)$ forms a diagonal matrix with the vector λ on the diagonal.

The main computational step is the eigenvalue decomposition which requires $\mathcal{O}(k^3)$ time. The correctness of the procedure can be verified as in [AZHHL17, Lemma 3.1] and [Gar19b, Lemma 6].

Unit nuclear ball We want to find (η^*, S^*) that solves

$$\text{minimize } \|(\eta, S) - (\eta_0, S_0)\|_2, \quad \text{subject to } \eta + \|S\|_{\text{nuc}} \leq 1, \eta \geq 0.$$

The procedures are as follows:

1. Compute the singular value decomposition of $S_0 = U\Lambda_0V^\top$, where $\Lambda_0 \in \mathbb{S}_+^k$ is a diagonal matrix with diagonal $\vec{\lambda}_0 = (\lambda_1, \dots, \lambda_k)$.
2. Compute $(\eta^*, \vec{\lambda}^*) = \arg \min_{(\eta, \vec{\lambda}) \in \Delta^{k+1}} \|(\eta_0, \vec{\lambda}_0) - (\eta, \vec{\lambda})\|_2$.
3. Form $S^* = U\text{diag}(\vec{\lambda}^*)V^\top$. Here $\text{diag}(\vec{\lambda}^*)$ forms a diagonal matrix with the vector $\vec{\lambda}^*$ on the diagonal.

The main computational step is the singular value decomposition which requires $\mathcal{O}(k^3)$ time. The correctness of the procedure can be verified as in [AZHHL17, Lemma 3.1] and [Gar19b, Lemma 6].

B Examples, lemmas, tables, and Proofs for Section 3

B.1 Further discussion on strict complementarity

We give two additional remarks on the strict complementarity.

1. Traditionally, the boundary location condition $x \in \partial\Omega$ is not included in the definition of strict complementarity. We include this condition for two reasons: first, the extra location condition excludes the trivial case that the dual solution of (1) is 0, and x_\star in the interior of Ω , in which case FW can be proved to converges linearly [GH15]; second, as we shall see in Example B.1, such assumption ensures the robustness of the sparsity of x_\star .
2. Strict complementarity (without the boundary location condition) holds generically: more precisely, it holds for almost all c in our optimization problem (1), $\min_{x \in \Omega} g(\mathcal{A}x) + \langle c, x \rangle$, [DL11, Corollary 3.5].

Example B.1. Consider the problem

$$\min_{x \in \alpha \Delta^n} \frac{1}{2} \|x - e_1 - \frac{1}{n} \mathbf{1}\|^2.$$

Here $\mathbf{1}$ is the all one vector and $\alpha > 0$. If we set $\alpha = 1$, then $x_\star = e_1$ and the gradient $\nabla f(x_\star) = -\frac{1}{n} \mathbf{1}$. Hence we see that strict complementarity does not hold, using Lemma 11. In this case, even though $x_\star = e_1$ is sparse for $\alpha = 1$, the solution is no longer sparse when α is slightly larger than 1. Hence, we see a perturbation to the constraint can cause instability of the sparsity when strict complementarity fails.

B.2 Lemmas and tables for strict complementarity

In this section, we show that the gap quantity defined in Definition 4 is indeed positive when strict complementarity holds. We then present a table of summarizing the notations $\mathcal{F}(x_\star)$, $\mathcal{F}^c(x_\star)$, and the gap δ .

Here, for the group norm ball, we consider a general norm denoted as $\|\cdot\|$ which is not necessarily the Euclidean ℓ_2 norm. The dual norm of $\|\cdot\|$ is defined as $\|x\|_* = \max_{\|y\| \leq 1} \langle y, x \rangle$. We note here the group norm ball is assumed to have radius one.

Lemma 11. *When Ω is a polytope, group norm ball, spectrahedron, and nuclear norm ball, if strict complementarity holds for Problem (1), then the gap δ is positive. Moreover, we can characterize the gradient at the solution and the size of the gap in each case:*

- *Polytope: order the vertices $v \in \Omega$ according to the inner products $\langle \nabla f(x_\star), v \rangle$ in ascending order as $v_1, \dots, v_{r_\star}, \dots, v_l$ where l is the total number of vertices. Then $\langle \nabla f(x_\star), v_i \rangle$, $i = 1, \dots, r_\star$ are all equal and the gap δ is $\delta = \langle \nabla f(x_\star), v_{r_\star+1} \rangle - \langle \nabla f(x_\star), v_{r_\star} \rangle$.*
- *Group norm ball for arbitrary base norm: order vectors $[\nabla f(x_\star)]_g$, $g \in \mathcal{G}$ according to their dual norm in descending order as $[\nabla f(x_\star)]_{g_1}, \dots, [\nabla f(x_\star)]_{g_{|\mathcal{G}|}}$. Then $\|[\nabla f]_{g_i}\|_*$, $i = 1, \dots, r_\star$ are all equal, and the gap δ is $\delta = \|[\nabla f(x_\star)]_{g_{r_\star}}\|_* - \|[\nabla f(x_\star)]_{g_{r_\star+1}}\|_*$.*
- *Spectrahedron: The smallest r_\star eigenvalues of $\nabla f(X_\star)$ are all equal and $\delta = \lambda_{n-r_\star}(\nabla f(X_\star)) - \lambda_{n-r_\star+1}(\nabla f(X_\star))$.*
- *Nuclear norm ball: The largest r_\star singular values of $\nabla f(X_\star)$ are all equal and $\delta = \sigma_{r_\star}(\nabla f(X_\star)) - \sigma_{r_\star+1}(\nabla f(X_\star))$.*

Proof. Let us first consider the polytope case.

Polytope. Since the constraint set is a polytope and $x_\star \in \partial\Omega$, we know the smallest face $\mathcal{F}(x_\star)$ containing x is proper and admits a face-defining inequality $\langle a, x \rangle \leq b$ for some $a \in \mathbb{R}^n$ and $b \in \mathbb{R}$. That is, $\mathcal{F}(x_\star) = \{x \mid \langle a, x \rangle = b\} \cap \Omega$ and for every $x \in \Omega$, $\langle a, x \rangle \leq b$. In particular, this implies that (1) for any vertex v that is not in $\mathcal{F}(x_\star)$, $\langle a, v \rangle < b$, and (2) $\langle a, x_\star \rangle = b$.

Let us now characterize the normal cone $N_\Omega(x_\star)$. Let \mathcal{V} be the set of vertices in Ω . Since Ω is bounded, we know that every point in Ω is a convex combination of the vertices. Hence $N_\Omega(x_\star)$ is the set of solutions g to the following linear system:

$$\langle g, v \rangle \leq \langle g, x_\star \rangle, \quad \text{for all } v \in \mathcal{V}. \quad (19)$$

Since $\mathcal{F}(x_\star)$ is the smallest face containing x_\star , we know that $x_\star \in \text{relint}(\mathcal{F}(x_\star))$, and so the description of normal cone $N_\Omega(x_\star)$ in (19) reduces to

$$\langle g, v_1 \rangle = \langle g, x_\star \rangle, \quad \text{for all } v_1 \in \mathcal{F}(x_\star), \quad (20)$$

$$\langle g, v_2 \rangle \leq \langle g, x_\star \rangle, \quad \text{for all } v_2 \text{ being vertices of } \mathcal{F}^c(x_\star). \quad (21)$$

Note that the vector a in the face-defining inequality satisfies (20) and satisfies (21) with strict inequality as we just argued. Hence, the relative interior of $N_\Omega(x_\star)$ consists of those vectors g that satisfy (20) and satisfy (21) with a strict inequality. As $-\nabla f(x_\star) \in \text{relint}(N_\Omega(x_\star))$, we know by the previous argument that $-\nabla f(x_\star)$ satisfies (21) with strict inequality, which is exactly the condition $\delta > 0$. We arrive at the formula for δ by noting that $\langle \nabla f(x_\star), v \rangle = \langle \nabla f(x_\star), x_\star \rangle$ for every $v \in \mathcal{F}(x_\star)$ due to (20).

Group norm ball. Again, recall we here define the group norm ball using any general norm $\|\cdot\|$. The normal cone at x_\star for unit group norm ball is defined as

$$N_\Omega(x_\star) = \{y \mid \langle y, x \rangle \leq \langle y, x_\star \rangle, \text{ for all } \sum_{g \in \mathcal{G}} \|x_g\| \leq 1\}.$$

Standard convex calculus reveals the following properties:

1. The normal cone is a linear multiple of the subdifferential for $x_\star \in \partial\Omega$: $N_\Omega(x_\star) = \{y \mid y \in \lambda \partial \|x_\star\|_{\mathcal{G}}, \lambda \geq 0\}$.
2. The product rule applies to $\partial \|x_\star\|_{\mathcal{G}}$ as \mathcal{G} forms a partition: $\partial \|x_\star\|_{\mathcal{G}} = \prod_{g \in \mathcal{G}} \partial \|(x_\star)_g\|$.
3. Any vector in the subdifferential of a group g in the support of the solution has norm 1: for every $g \in \mathcal{F}(x_\star)$ and every $y_g \in \partial \|(x_\star)_g\|$, $\|y_g\|_* = 1$, and $\langle y_g, (x_\star)_g \rangle = \|(x_\star)_g\|$.
4. The subdifferential for groups g not in the support is a unit dual norm ball: for every $g \notin \mathcal{F}(x_\star)$, $\partial \|(x_\star)_g\| = \mathbf{B}_{\|\cdot\|_*} := \{y_g \in \mathbb{R}^{|g|} \mid \|y_g\|_* \leq 1\}$.

The above properties reveal that the normal cone is the set

$$N_\Omega(x_\star) = \left\{ y \mid y \in \lambda \left(\prod_{g \in \mathcal{F}(x_\star)} \partial \|(x_\star)_g\| \times \prod_{g \in \mathcal{G} \setminus \mathcal{F}(x_\star)} \mathbf{B}_{\|\cdot\|_*} \right), \lambda \geq 0 \right\}, \quad (22)$$

where for every $g \in \mathcal{F}(x_\star)$ and every $y_g \in \partial \|(x_\star)_g\|$, $\|y_g\|_* = 1$. Hence, we know that the relative interior of $N_\Omega(x_\star)$ is simply

$$\begin{aligned} & \text{relint}(N_\Omega(x_\star)) \\ &= \left\{ y \mid y \in \lambda \left(\prod_{g \in \mathcal{F}(x_\star)} \text{relint}(\partial \|(x_\star)_g\|) \times \prod_{g \in \mathcal{G} \setminus \mathcal{F}(x_\star)} \text{relint}(\mathbf{B}_{\|\cdot\|_*}) \right), \lambda > 0 \right\}, \end{aligned} \quad (23)$$

where for every $g \in \mathcal{F}(x_*)$, and every $y_g \in \text{relint}(\partial\|(x_*)_g\|)$, $\|y_g\|_* = 1$, and for every $g \in \mathcal{G} - \mathcal{F}(x_*)$, and every $y_g \in \text{relint}(\mathbf{B}_{\|\cdot\|_*})$, $\|y_g\|_* < 1$. Because of the strict inequality of λ in (23), and strict inequality for $\|y_g\|_* < 1$ for $y_g \in \text{relint}(\mathbf{B}_{\|\cdot\|_*})$, we see that

$$\begin{aligned} \|\nabla f(x_*)\|_{g_1} &= \dots = \|\nabla f(x_*)\|_{g_{r_*}} \|_*, \text{ and} \\ \|\nabla f(x_*)\|_{g_{r_*}} \|_* &- \|\nabla f(x_*)\|_{g_{r_*+1}} \|_* > 0 \end{aligned} \quad (24)$$

as $-\nabla f(x_*) \in \text{relint}(N_\Omega(x_*))$. Using the condition that for every $g \in \mathcal{F}(x_*)$ and every $y_g \in \partial\|(x_*)_g\|$, $\|y_g\|_* = 1$, and $\langle y_g, (x_*)_g \rangle = \|(x_*)_g\|$, we know $\langle -\nabla f(x_*), x_* \rangle = \|\nabla f(x_*)\|_{g_{r_*}} \|_*$. Furthermore, using generalized Cauchy-Schwarz, it can be proved that $\min_{x \in \mathcal{F}^c(x_*)} \langle \nabla f(x_*), x \rangle = -\|\nabla f(x_*)\|_{g_{r_*+1}} \|_*$. Hence, combining the two equalities with (24), we see that $\delta > 0$ and arrive at the stated formula for δ .

Spectrahedron. We first note that $X_* \in \partial\Omega$ and $\text{tr}(X) = 1$ imply that $1 \leq r_* < n$. To compute the normal cone, we can apply the sum rule of subdifferentials to

$$\chi(\{X \in \mathbb{S}^n \mid \text{tr}(X) = 1\}) + \chi(X \succeq 0),$$

where χ is the characteristic function, which takes value 0 for elements belonging to the set and $+\infty$ otherwise) of $\{X \in \mathbb{S}^n \mid \text{tr}(X) = 1\}$ and \mathbb{S}_+^n and reach

$$N_\Omega(X_*) = \{sI \mid s \in \mathbb{R}\} + \{-Z \mid Z \succeq 0, \text{range}(Z) \subseteq \text{nullspace}(X_*)\}. \quad (25)$$

We note that the sum rule for the relative interior is valid here because $\frac{1}{n}I$ belongs to the interior of both sets. Applying the sum rule to (25), we find that

$$\text{relint}(N_\Omega(X_*)) = \{sI \mid s \in \mathbb{R}\} + \{-Z \mid Z \succeq 0, \text{range}(Z) = \text{nullspace}(X_*)\}.$$

Or equivalently,

$$\text{relint}(N_\Omega(X_*)) = \{sI \mid s \in \mathbb{R}\} + \{-Z \mid Z \succeq 0, \text{nullspace}(Z) = \text{range}(X_*)\}.$$

Using the above equality and $-\nabla f(X_*) \in \text{relint}(N_\Omega(X_*))$, we know there are $Z_* \succeq 0$ and $s_* \in \mathbb{R}$ that

$$\nabla f(X_*) = -s_*I + Z_*, \text{ and } \text{nullspace}(Z_*) = \text{range}(X_*). \quad (26)$$

Denote the eigenspace corresponding to the smallest r_* values of $\nabla f(X_*)$ as $\mathbf{EV}_{r_*}(\nabla f(X_*))$. From (26), it is immediate that

$$\mathbf{EV}_{r_*}(\nabla f(X_*)) = \text{range}(X_*).$$

Moreover, from (26), we also have

$$\begin{aligned} \lambda_{n-r_*+1}(\nabla f(X_*)) - \lambda_{n-r_*}(\nabla f(X_*)) &> 0, \quad \text{and} \\ \langle \nabla f(X_*), X_* \rangle &= -s_* = \lambda_{n-i+1}(\nabla f(X_*)), \quad i = 1, \dots, r_*. \end{aligned} \quad (27)$$

Combining (27) and the well-known fact that

$$\min_{X \in \Omega, \text{range}(X) \perp \mathbf{EV}_{r_*}(\nabla f(X_*))} \langle \nabla f(X_*), X \rangle = \lambda_{n-r_*+1}(\nabla f(X_*)),$$

we see that δ is indeed positive, and the formula for δ holds.

Nuclear norm ball. We first note that $X_\star \in \partial\Omega$ imply that $1 < r_\star < \min(n_1, n_2)$, and $\|X_\star\|_{\text{nuc}} = 1$. Let the singular value decomposition of X_\star as $X_\star = U\Sigma V$ with $U \in \mathbb{R}^{n_1 \times r_\star}$ and $V \in \mathbb{R}^{n_2 \times r_\star}$. The normal cone of the unit nuclear norm ball is

$$N_\Omega(X_\star) = \{Y \mid Y = \lambda Z, Z = UV^\top + W, W^\top U = 0, WV = 0, \|W\|_{\text{op}} \leq 1 \text{ and } \lambda \geq 0\}. \quad (28)$$

Hence, the relative interior is

$$N_\Omega(X_\star) = \{Y \mid Y = \lambda Z, Z = UV^\top + W, W^\top U = 0, WV = 0, \|W\|_{\text{op}} < 1 \text{ and } \lambda > 0\}. \quad (29)$$

Since $-\nabla f(X_\star) \in \text{relint}(N_\Omega(X_\star))$, we know immediately that

$$\sigma_{r_\star}(\nabla f(X_\star)) - \sigma_{r_\star+1}(\nabla f(X_\star)) > 0, \quad (30)$$

and the top r_\star left and right singular vectors of $\nabla f(X_\star)$ are just the columns of $-U$ and V , and $\langle \nabla f(X_\star), X_\star \rangle = -\sigma_i(\nabla f(X_\star))$ for $i = 1, \dots, r_\star$. Combining pieces and the standard fact that

$$\min_{\text{range}(X) \perp \text{range}(U), \|X\|_{\text{nuc}} \leq 1} \langle \nabla f(X_\star), X \rangle = -\sigma_{r_\star+1}(\nabla f(X_\star)),$$

we see the gap δ is indeed positive and the formula is correct. \square

A table of the notions $\mathcal{F}(x_\star)$, $\mathcal{F}^c(x_\star)$, and the formula of gap δ is shown as Table 8.

Table 8: For several constraint sets Ω , this table describes the support set $\mathcal{F}(x_\star)$, its complementary set \mathcal{F}^c , and the gap $\delta = \min\{\langle u, \nabla f(x_\star) \rangle - \langle x_\star, \nabla f(x_\star) \rangle \mid u \in \mathcal{F}^c(x_\star) \subseteq \Omega\}$ and admits a specific formula as described in Lemma 11. We denote the gradient at x_\star as ∇_\star . For a polytope, we order the vertices $v \in \Omega$ according to their inner products $\langle \nabla f(x_\star), v \rangle$ in ascending order as $v_1, \dots, v_{r_\star}, \dots, v_l$, where l is the number of vertices. For the group norm ball, we order vectors $[\nabla f(x_\star)]_g, g \in \mathcal{G}$ according to their ℓ_2 norm in descending order as $[\nabla f(x_\star)]_{g_1}, \dots, [\nabla f(x_\star)]_{g_{|\mathcal{G}|}}$.

Constraint Ω	$\mathcal{F}(x_\star)$	\mathcal{F}^c	δ formula
polytope	smallest face containing x_\star	convex hull of all the vertices not in $\mathcal{F}(x_\star)$	$\langle \nabla f(x_\star), v_{r_\star+1} \rangle$ $-\langle \nabla f(x_\star), v_{r_\star} \rangle$
group norm ball	$\{g \in \mathcal{G} \mid (x_\star)_g \neq 0\}$	$\{x \mid x_g = 0, \forall g \in \mathcal{F}(x_\star)\}$	$\ [\nabla_\star]_{g_{r_\star}}\ _2$ $-\ [\nabla_\star]_{g_{r_\star+1}}\ _2$
Spectrahedron	$\text{range}(X_\star)$	$\{X \in [\text{range}(X_\star)]^\perp\} \cap \mathcal{SP}^n$	$\lambda_{n-r_\star}(\nabla_\star)$ $-\lambda_{n-r_\star+1}(\nabla_\star)$
Nuclear norm ball	$\text{range}(X_\star)$	$\{X \in [\text{range}(X_\star)]^\perp\} \cap \mathbf{B}_{\ \cdot\ _{\text{nuc}}}$	$\sigma_{r_\star}(\nabla_\star)$ $-\sigma_{r_\star+1}(\nabla_\star)$

B.3 Quadratic growth under strict complementarity

This section develops that quadratic growth does hold under strict complementarity and the condition g in (1) is strongly convex.

Theorem 12. *Suppose Problem (1), $\min_{x \in \Omega} g(\mathcal{A}x) + \langle c, x \rangle$, satisfies that g is strongly convex and the constraint set Ω is one of the four sets (i) polytope, (ii) unit group norm ball, (iii) spectrahedron, and (vi) unit nuclear norm ball. Further suppose that strict complementarity holds. Then quadratic growth holds for Problem (1) as well.*

We will use the machinery developed in [ZS17] for the case of the group norm. We define a few notions and notations for later convenience. We define the projection to Ω as $\mathcal{P}_\Omega(x) := \arg \min_{v \in \Omega} \|x - v\|_2$. The difference of iterates for projected gradient with step size t is defined as $\mathcal{G}_t(x) := \frac{1}{t}(x - \mathcal{P}_\Omega(x - \nabla f(x)))$. Note that $\mathcal{G}_t(x) = 0$ implies $x = x_*$. Finally, for an arbitrary set \mathcal{S} , we define the distance of $x \in \mathbb{R}^n$ to it as $\text{dist}(x, \mathcal{S}) := \inf_{v \in \mathcal{S}} \|x - v\|_2$.

Proof. The proof for the polytope appears in [BS17, Lemma 2.5]. The proof of the Spectrahedron appears in [DFXY20, Theorem 6]. Here, we address the case of the group norm ball and Nuclear norm ball. Let us first consider the case of the group norm ball with the ℓ_2 norm.

Unit group norm ball. Using [DL18, Corollary 3.6], we know that if the error bound condition holds for some $t, \gamma > 0$ then the quadratic growth condition holds with some parameter γ' . The error bound condition with parameter $t, \gamma, \epsilon > 0$ means that for all $x \in \Omega$ and $\|x - x_*\|_2 \leq \epsilon$, the following inequality holds:⁸

$$\|x - x_*\|_2 \leq \gamma \|\mathcal{G}_t(x)\|_2. \quad (31)$$

Define $\bar{y} = \mathcal{A}(x_*)$ and $\bar{h} = \nabla f(x_*)$. Now using [ZS17, Corollary 1 and Theorem 2], we need only verify the following two conditions to establish (31):

1. *Bounded linear regularity:* The two sets $\Gamma_f(\bar{y}) := \{x \in \mathbf{E} \mid \bar{y} = \mathcal{A}(x)\}$ and $\Gamma_\Omega(\bar{h}) := \{x \in \mathbf{E} \mid -\bar{h} \in N_\Omega(x)\}$ satisfy that for every bounded set B , there exists a constant κ such that

$$\text{dist}(x, \Gamma_f(\bar{y}) \cap \Gamma_\Omega(\bar{h})) \leq \kappa \max\{\text{dist}(x, \Gamma_f(\bar{y})), \text{dist}(x, \Gamma_\Omega(\bar{h}))\}, \text{ for all } x \in \Omega.$$

2. *Metric subregularity:* there exists $\kappa, \epsilon > 0$ such that for all x with $\|x - x_*\|_2 \leq \epsilon$,

$$\text{dist}(x, \Gamma_\Omega(\bar{h})) \leq \kappa \text{dist}(-\bar{h}, N_\Omega(x)). \quad (32)$$

Let us first verify bounded linear regularity. First, the subdifferential of the Euclidean norm $\|\cdot\|_2$ is

$$\partial\|x\|_2 = \begin{cases} \frac{x}{\|x\|_2} & x \neq 0, \\ \mathbf{B}_{\|\cdot\|_2} & x = 0. \end{cases}$$

Here $\mathbf{B}_{\|\cdot\|_2} := \{x \mid \|x\|_2 \leq 1\}$ is unit ℓ_2 norm ball.

From the characterization (23) of the interior of the normal cone, we know that $\bar{h} = \nabla f(x_*)$ is nonzero due to strict complementarity, and hence any $x \in \Gamma(\bar{h})$ must satisfy $x \in \partial\Omega$. Following the derivation of the normal cone in (22), we have for any $x \in \partial\Omega$,

$$N_\Omega(x) = \left\{ y \mid y \in \lambda \left(\prod_{g \in \mathcal{F}(x)} \partial\|x_g\|_2 \times \prod_{g \in \mathcal{G} - \mathcal{F}(x)} \mathbf{B}_{\|\cdot\|_2} \right), \lambda \geq 0 \right\}. \quad (33)$$

Here the support set $\mathcal{F}(x)$ is the set of groups in the support of x . Let us pick a $i^* \in \mathcal{F}(x_*)$. For each $i \in \mathcal{G}$, define the vector $\tilde{h}_i = \frac{-\bar{h}_i}{\|\bar{h}_{i^*}\|_2} \in \mathbb{R}^{|v_i|}$. Recall from (24), we have $\|\bar{h}_i\|_2$ all equal for

⁸The error bound condition considered in [DL18, Corollary 3.6] actually require the bound (31) to hold for all x in the intersection of Ω and a sublevel set of f . Note there is a difference between a sublevel set and a neighborhood of x_* . However, as f is continuous and Ω is compact, when restricted to Ω any neighborhood of x_* is contained in a sublevel set and vice versa. Moreover, the quadratic growth condition of [DL18, Corollary 3.6] is only required to hold for x in Ω and a sublevel set of f . Again, this condition is equivalent to ours as to Ω is compact and f is continuous.

$i \in \mathcal{F}(x_*)$. For each $i \in \mathcal{F}(x_*)$, define $\tilde{h}^i \in \mathbb{R}^n$ so that it is only supported on group i with vector value \tilde{h}_i and is 0 elsewhere. Again, from (24) and Lemma 11, we have $\|\tilde{h}^i\|_2$ all equal for $i \in \mathcal{F}(x_*)$, and is larger than those i not in $\mathcal{F}(x_*)$. To remember the notation, we use \tilde{h}^i , upper index i , to mean a vector in \mathbb{R}^n . We use the notation \tilde{h}_i , lower index i , to mean the shorter vector in $\mathbb{R}^{|v_i|}$.

Combining the facts about \tilde{h}_i , the formula (33), the formula of $\partial\|\cdot\|_2$, and $x \in \partial\Omega$, we find that actually

$$\Gamma_\Omega(\bar{h}) = \{x \mid \sum_{i \in \mathcal{F}(x_*)} \alpha_i \tilde{h}^i, \alpha_i \in \Delta^{|\mathcal{F}(x_*)|}\},$$

which is a convex polyhedral. Because $\Gamma_f(\bar{y})$ and $\Gamma_\Omega(\bar{h})$ are both convex polyhedral, we know from [BBL99, Corollary 3] that bounded linear regularity holds.

We verify metrical subregularity now. Note that from previous calculation of $\Gamma_\Omega(\bar{h})$, we know

$$\text{dist}(x, \Gamma_\Omega(\bar{h}))^2 = \min_{\alpha_i \in \Delta^{|\mathcal{F}(x_*)|}} \sum_{i \in \mathcal{F}(x_*)} \|x_i - \alpha_i \tilde{h}_i\|_2^2 + \sum_{i \notin \mathcal{F}(x_*)} \|x_i\|_2^2.$$

By choosing ϵ sufficiently small, say $\epsilon < \epsilon_0$, we have $\mathcal{F}(x) \supseteq \mathcal{F}(x_*)$. The quantity, $\text{dist}(\bar{h}, N_\Omega(x))$, on the RHS of (32) for all x within an ϵ neighborhood of the solution x_* satisfies that

$$\text{dist}^2(\bar{h}, N_\Omega(x)) = \begin{cases} +\infty, & x \notin \Omega, \\ \|\bar{h}\|_2^2, & x \in \text{int}(\Omega), \end{cases}$$

where $\text{int}(\Omega)$ is the interior of Ω . For $x \in \partial\Omega$, $\text{dist}^2(\bar{h}, N_\Omega(x))$ satisfies that

$$\text{dist}^2(\bar{h}, N_\Omega(x)) = \|h_{i^*}\|_2^2 \min_{\lambda \geq 0, v_i \in \mathbf{B}_{\|\cdot\|_2}} \sum_{i \in \mathcal{F}(x)} \|\tilde{h}_i - \lambda \tilde{x}_i\|_2^2 + \sum_{i \notin \mathcal{F}(x)} \|\tilde{h}_i - \lambda v_i\|_2^2,$$

where $\tilde{x} = \frac{x}{\|x\|_2}$, and \tilde{x}_i is the vector with components in group i . The case of $x \notin \Omega$ is trivial. The case of $x \in \text{int}(\Omega)$ can be proved by choosing a large enough κ , say $\kappa > K_0$, as $\text{dist}(x, \Gamma_\Omega(\bar{h}))^2$ is upper bounded for any $x \in \text{int}(\Omega)$, and $\text{dist}^2(\bar{h}, N_\Omega(x))$ in this case is fixed. We are left with the most challenging case $x \in \partial\Omega$, where the normal cone is non-trivial. First, we upper bound $\text{dist}(x, \Gamma_\Omega(\bar{h}))^2$ by choosing $\alpha_i = \|x_i\|_2$. The numbers α_i sum to one because $x \in \partial\Omega$. In this case, $\text{dist}(x, \Gamma_\Omega(\bar{h}))^2$ satisfies the bound

$$\begin{aligned} \text{dist}(x, \Gamma_\Omega(\bar{h}))^2 &\leq \sum_{i \in \mathcal{F}(x_*)} \|x_i - \|x_i\|_2 \tilde{h}_i\|_2^2 + \sum_{i \notin \mathcal{F}(x_*)} \|x_i\|_2^2 \\ &\stackrel{(a)}{=} \sum_{i \in \mathcal{F}(x_*)} \|x_i\|_2 \|\tilde{h}_i - \tilde{x}_i\|_2^2 + \sum_{i \in (\mathcal{F}(x) - \mathcal{F}(x_*))} \|x_i\|_2^2, \end{aligned} \tag{34}$$

where step (a) is due to $\mathcal{F}(x) \supseteq \mathcal{F}(x_*)$ by our choice of small enough ϵ . We next lower bound $\text{dist}^2(\bar{h}, N_\Omega(x))$ by ignoring the term not in $\mathcal{F}(x)$:

$$\text{dist}^2(\bar{h}, N_\Omega(x)) \geq \|g_{i^*}\|_2^2 \min_{\lambda \geq 0} \sum_{i \in \mathcal{F}(x)} \|\tilde{h}_i - \lambda \tilde{x}_i\|_2^2$$

Now if $\mathcal{F}(x) = \mathcal{F}(x_*)$, then it is tempting to set $\lambda = 1$ above and compare the inequality with (34) to claim victory. This does not work directly due to the minimization over λ and the fact $\mathcal{F}(x) \supseteq \mathcal{F}(x_*)$.

Let $\lambda_\star = \arg \min_{\lambda \geq 0} \sum_{i \in \mathcal{F}(x)} \|\tilde{h}_i - \frac{\lambda x_i}{\|x_i\|_2}\|_2^2$. In this case, we have an explicit formula of λ_\star :

$$\lambda_\star = \max \left\{ 0, \frac{\sum_{i \in \mathcal{F}(x)} \langle \tilde{h}_i, \tilde{x}_i \rangle}{|\mathcal{F}(x)|} \right\}.$$

If $\lambda_\star = 0$, then we can simply pick some $\kappa > K_0$ as done in the case of $x \in \text{int}(\Omega)$. So we assume $\lambda_\star > 0$ in the following. Next let $\lambda_i = \arg \min_{\lambda \geq 0} \|\tilde{h}_i - \frac{\lambda x_i}{\|x_i\|_2}\|_2^2$ for each $i \in \mathcal{F}(x_\star)$. With such choice of λ_i and λ_\star , we can further lower bound $\text{dist}^2(\bar{h}, N_\Omega(x))$ by splitting the terms in $\mathcal{F}(x)$ and those are not:

$$\text{dist}^2(\bar{h}, N_\Omega(x)) \geq \|g_{i^\star}\|_2^2 \left(\underbrace{\sum_{i \in \mathcal{F}(x_\star)} \|\tilde{h}_i - \frac{\lambda_i x_i}{\|x_i\|_2}\|_2^2}_{R_1} + \underbrace{\sum_{i \in \mathcal{F}(x) \setminus \mathcal{F}(x_\star)} \|\tilde{h}_i - \frac{\lambda_\star x_i}{\|x_i\|_2}\|_2^2}_{R_2} \right). \quad (35)$$

We bound the two terms separately. Let us first deal with R_1 . From the expression of normal cone (33) and $-\bar{h} \in N_\Omega(x_\star)$ by our assumption, we know $\tilde{h}_i = \frac{(x_\star)_i}{\|(x_\star)_i\|_2}$ for every $i \in \mathcal{F}(x_\star)$. Hence by choosing a (possibly smaller) ϵ , say $\epsilon < \epsilon_1$, we can ensure that for any x within an ϵ_1 neighborhood of the solution x_\star , $\langle \tilde{x}_i, \tilde{h}_i \rangle \geq 0$ all for $i \in \mathcal{F}(x_\star)$. Moreover, for a small enough ϵ_1 , we know each $\lambda_i = \langle \tilde{x}_i, \tilde{h}_i \rangle$ and is very close to 1. Thus the condition of Lemma 13 is fulfilled, and we have

$$R_1 \geq \frac{1}{2} \sum_{i \in \mathcal{F}(x_\star)} \|x_i\|_2 \|\tilde{h}_i - \tilde{x}_i\|_2^2. \quad (36)$$

Next, to deal with R_2 , let us examine the expression of $\lambda_\star = \frac{\sum_{i \in \mathcal{F}(x)} \langle \tilde{h}_i, \tilde{x}_i \rangle}{|\mathcal{F}(x)|}$. Recall $\langle \tilde{h}_i, \tilde{x}_i \rangle$ is close to 1 for small enough ϵ . Due to strict complementarity, for each $i \in \mathcal{F}(x) \setminus \mathcal{F}(x_\star)$, we know $\|\tilde{h}_i\|_2 < 1 - \delta_0$ for some $\delta_0 > 0$ that depends only on \bar{h} . Combining these two facts, we know that $i' = \arg \min_{i \in \mathcal{F}(x)} \langle \tilde{h}_i, \tilde{x}_i \rangle$ must belong to $\mathcal{F}(x) \setminus \mathcal{F}(x_\star)$. Moreover, by choosing an even smaller ϵ , say $\epsilon < \epsilon_2$, we have $\lambda_\star \geq \delta_1 + \min_i \langle \tilde{h}_i, \tilde{x}_i \rangle$ for some $\delta_1 > 0$ that only depends on \bar{h} , δ , and ϵ_2 . We can now lower bound R_2 as follows:

$$\begin{aligned} R_2 &\geq \|\tilde{h}_{i'} - (\delta_1 + \langle \tilde{h}_i, \tilde{x}_i \rangle) \tilde{x}_{i'}\|_2^2 \\ &= \|\tilde{h}_i - \langle \tilde{h}_i, \tilde{x}_i \rangle \tilde{x}_{i'}\|_2^2 + \delta_1^2 \\ &\quad + 2\delta \underbrace{\langle \tilde{h}_i - \langle \tilde{h}_i, \tilde{x}_i \rangle \tilde{x}_{i'}, \tilde{x}_{i'} \rangle}_{=0} \\ &\geq \delta_1^2. \end{aligned} \quad (37)$$

Combining the bounds (36) and (37) on R_1 and R_2 , we find that

$$\begin{aligned} \text{dist}^2(\bar{h}, N_\Omega(x)) &\geq \frac{\|g_{i^\star}\|_2^2}{2} \sum_{i \in \mathcal{F}(x_\star)} \|\tilde{h}_i - \tilde{x}_i\|_2^2 + \|g_{i^\star}\|_2^2 \delta_1^2 \\ &\stackrel{(a)}{\geq} \frac{\|g_{i^\star}\|_2^2}{2} \sum_{i \in \mathcal{F}(x_\star)} \|x_i\|_2 \|\tilde{h}_i - \tilde{x}_i\|_2^2 + \|g_{i^\star}\|_2^2 \delta_1^2 \sum_{i \in \mathcal{F}(x) \setminus \mathcal{F}(x_\star)} \|x_i\|_2^2 \end{aligned} \quad (38)$$

Here, for the step (a), we use $\|x_i\|_2 \leq 1$ as $x \in \partial\Omega$. Hence, by taking $\epsilon = \min(\epsilon_1, \epsilon_2)$ and $\kappa = \max\{K_0, \|g_{i^\star}\|_2^2 \delta_1, \frac{\|g_{i^\star}\|_2^2}{2}\}$, and comparing (38) with (34), a bound on $\text{dist}(x, \Gamma_\Omega(\bar{h}))^2$, we see that metric subregularity is satisfied and our proof for unit group norm ball is complete.

Finally, we consider the unit nuclear norm ball.

Unit nuclear norm ball. Let us first illustrate the main idea. We shall utilize the quadratic growth result proved in [DFXY20, Theorem 6] for spectrahedron. To transfer our setting to spectrahedron, we use a dilation argument with its relating lemmas [DU20, Lemma 3] and [JS10, lemma 1]. We now spell out all the details.

Let $\tilde{n} = n_1 + n_2$. For any $\tilde{X} \in \mathbb{S}^{\tilde{n}}$, denote its eigenvalues as $\lambda_1(\tilde{X}) \geq \dots \geq \lambda_{\tilde{n}}(\tilde{X})$. Also, for any $X \in \mathbf{B}_{\|\cdot\|_{\text{nuc}}}$, denote its singular value decomposition as $X = U_X \Sigma_X V_X^\top$ where $U_X \in \mathbb{R}^{n_1 \times r_X}$, $V_X \in \mathbb{R}^{n_2 \times r_X}$, and $r_X = \text{rank}(X)$. Define the dilation $X^\sharp \in \mathbb{S}^{\tilde{n}}$ of a $X \in \mathbb{R}^{n_1 \times n_2}$ as

$$X^\sharp = \frac{1}{2} \begin{bmatrix} X_1 & X \\ X^\top & X_2 \end{bmatrix}, \quad (39)$$

where the $X_1 = U_X(\Sigma_X + \xi_X I)U_X^\top$, and $X_2 = V_X(\Sigma_X + \xi_X I)V_X^\top$. The number $\xi_X \geq 0$ is chosen so that X^\sharp has trace 1. Note that X^\sharp is positive semidefinite as $X^\sharp = \frac{1}{2} \begin{bmatrix} U_X \\ V_X \end{bmatrix} \Sigma_X [U_X^\top \ V_X^\top] + \frac{\xi_X}{2} \begin{bmatrix} U_X U_X^\top & 0 \\ 0 & V_X V_X^\top \end{bmatrix}$. For any $\tilde{Y} = \frac{1}{2} \begin{bmatrix} Y_1 & Y \\ Y^\top & Y_2 \end{bmatrix} \in \mathbb{S}^{\tilde{n}}$ with $Y_1 \in \mathbb{S}^{n_1}$, and $Y_2 \in \mathbb{S}^{n_2}$, we denote its off diagonal component as

$$\tilde{Y}_b := Y.$$

Note here that X^\sharp denotes the dilation of a matrix $X \in \mathbb{R}^{n_1 \times n_2}$, while \tilde{X} means a generic matrix in $\mathbb{S}^{\tilde{n}}$ which is not necessarily related to X . We also have the relation that $(X^\sharp)_b = X$ for any $X \in \mathbb{R}^{n_1 \times n_2}$.

Consider the problem

$$\begin{aligned} & \text{minimize} && \tilde{f}(\tilde{X}) := f(\tilde{X}_b) = g(\mathcal{A}(\tilde{X}_b)) + \langle C, (\tilde{X})_b \rangle \\ & \text{subject to} && \tilde{X} = 1 \quad \tilde{X} \succeq 0. \end{aligned} \quad (40)$$

We claim that it satisfies strict complementarity and its solution \tilde{X}_\star is unique and is equal to X_\star^\sharp . Suppose the claim is proved for the moment. Note that $X_\star \in \partial\Omega$ implies that $\text{rank}(X_\star^\sharp) = \text{rank}(X_\star) < \tilde{n}$. Hence, the condition of [DFXY20, Theorem 6] is fulfilled, and we know there is some $\tilde{\gamma} > 0$, such that for all $\tilde{X} \in \mathcal{SP}^{\tilde{n}}$, we have

$$\tilde{f}(\tilde{X}) - \tilde{f}(X_\star^\sharp) \geq \tilde{\gamma} \|\tilde{X} - X_\star^\sharp\|_{\text{F}}.$$

Hence, for any $X \in \Omega$, by construction of \tilde{f} , we have

$$f(X) - f(X_\star) = \tilde{f}(X^\sharp) - \tilde{f}(X_\star^\sharp) \geq \tilde{\gamma} \|X^\sharp - X_\star^\sharp\|_{\text{F}}^2 \geq \frac{\tilde{\gamma}}{2} \|X - X_\star\|_{\text{F}}^2.$$

This proves quadratic growth.

We now verify our claim that X_\star^\sharp is the unique solution to (40) and $X_\star^\sharp \in \partial\mathcal{SP}^{\tilde{n}}$ with $\nabla \tilde{f}(X_\star^\sharp) \in \partial N_{\mathcal{SP}^{\tilde{n}}}(X_\star^\sharp)$. First, consider feasibility and whether $X_\star^\sharp \in \partial\mathcal{SP}^{\tilde{n}}$. The condition $X_\star \in \partial\Omega$ implies that $1 \leq r_\star < \min(n_1, n_2)$ and $\|X_\star\|_{\text{nuc}} = 1$. Hence we do have $\text{tr}(X_\star^\sharp) = 1$ and $X_\star^\sharp \in \partial\mathcal{SP}^{\tilde{n}}$ as $\text{rank}(X_\star^\sharp) = \text{rank}(X_\star) = r_\star < n_1 + n_2$. Next, consider optimality. Given any $\tilde{X} \in \mathcal{SP}^{\tilde{n}}$, we may write it as $\tilde{X} = \frac{1}{2} \begin{bmatrix} X_1 & X \\ X^\top & X_2 \end{bmatrix}$. By [JS10, Lemma 1], we have

$$\|X\|_{\text{nuc}} \leq 1. \quad (41)$$

To see X_\star^\sharp is optimal for (40), note that

$$f((\tilde{X})_b) = f(X) \stackrel{(a)}{\geq} f(X_\star) = f((X_\star^\sharp)_b),$$

where step (a) is due to optimality of X_\star in (1) and X is feasible as just argued. Thirdly, we argue that X_\star^\sharp is a unique solution to (40). For any optimal solution $\tilde{X}_\star = \frac{1}{2} \begin{bmatrix} X_\star^\dagger & X_0 \\ X_0^\top & X_\star^\star \end{bmatrix}$ of (40), we have X_0 is optimal to (1) as

$$f(X_0) = f((\tilde{X}_\star)_b) \stackrel{(a)}{=} f((X_\star^\sharp)_b) = f(X_\star),$$

where step (a) is because X_\star^\sharp is optimal to (40). Hence due to uniqueness of X_\star , we know $X_0 = X_\star$. Because $\|X_\star\|_{\text{nuc}} = 1$, using [DU20, Lemma 3], we know in fact $X_\star^\sharp = \tilde{X}_\star$ and uniqueness of solution to (40) is proved. Finally, we verify strict complementarity that $\nabla \tilde{f}(X_\star^\sharp) \in \text{relint}(N_{\mathcal{SP}^{\tilde{n}}}(X_\star^\sharp))$. Recall from (26), that we need to show

$$-\nabla \tilde{f}(X_\star^\sharp) \in \text{relint}(N_{\mathcal{SP}^{\tilde{n}}}(\tilde{X}_\star)) = \{sI \mid s \in \mathbb{R}\} + \{-\tilde{Z} \mid \tilde{Z} \succeq 0, \text{range}(\tilde{Z}) = \text{nullspace}(X_\star^\sharp)\}.$$

Using the definition of X_\star^\sharp , we know

$$\nabla \tilde{f}(X_\star^\sharp) = \begin{bmatrix} 0 & \nabla f(X_\star) \\ \nabla f(X_\star)^\top & 0 \end{bmatrix}.$$

Recall from Lemma 11, we have $\sigma_1(\nabla f(X_\star)) = \dots = \sigma_{r_\star}(\nabla f(X_\star)) = \delta + \sigma_{r_\star+1}(\nabla f(X_\star))$ for some gap $\delta > 0$. Hence we see that $\nabla \tilde{f}(X_\star^\sharp)$ has all its smallest r_\star eigenvalues equal as $-\sigma_{r_\star}(\nabla f(X_\star))$ and the gap between its r_\star -th smallest eigenvalue and the $r_\star + 1$ -th eigenvalue is simply $\delta > 0$. Moreover, let the singular value decomposition of X_\star as $X_\star = U_\star \Sigma V_\star^\top$ with $U_\star \in \mathbb{R}^{n_1 \times r_\star}$ and $V_\star \in \mathbb{R}^{n_2 \times r_\star}$. From the description of normal cone of nuclear norm ball in (29), we know $U_\star, -V_\star$ are the matrices formed by the top r_\star left and right vectors of $\nabla f(X_\star)$. Hence, the bottom r_\star eigenvector of $\nabla \tilde{f}(X_\star^\sharp)$ is simply $\frac{1}{\sqrt{2}} \begin{bmatrix} U_\star \\ V_\star \end{bmatrix}$. Since $\text{range}(X_\star^\sharp) = \text{range}\left(\begin{bmatrix} U_\star \\ V_\star \end{bmatrix}\right)$, we may take $s = \sigma_1(\nabla f(X_\star))$ and $\tilde{Z} = \sigma_1(\nabla f(X_\star))I + \nabla \tilde{f}(X_\star^\sharp)$. Using the eigengap condition on $\nabla \tilde{f}(X_\star^\sharp)$, we see $\text{range}(\tilde{Z}) = \text{nullspace}(X_\star^\sharp)$ and our claim is proved. \square

B.3.1 Additional Lemma for quadratic growth

We establish the following lemma for the proof of unit group norm ball.

Lemma 13. *For any two $x, y \in \mathbb{R}^d$ with ℓ_2 norm one, and $a := \langle x, y \rangle \geq 0$, we have*

$$2 \min_{\lambda \geq 0} \|x - \lambda y\|_2^2 \geq \|x - y\|_2^2.$$

Proof. Simple calculus reveals that the optimal solution λ^\star of the LHS of the inequality is $\lambda^\star = a \geq 0$. We know $a \in [0, 1]$ due to Cauchy-Schwarz and our assumption on a . Direct calculation of the difference yields

$$\begin{aligned} 2 \min_{\lambda \geq 0} \|x - \lambda y\|_2^2 - \|x - y\|_2^2 &= 2 + 2a^2 - 4a^2 - 2 + 2a \\ &= -2a^2 + 2a \geq 0, \end{aligned} \tag{42}$$

where the last line is due to $a \in [0, 1]$. \square

B.4 Proofs of Theorem 7 for group norm ball

Proof. Let us now consider Algorithm 2 whose constraint set Ω is a unit group norm ball with *arbitrary* base norm $\|\cdot\|$. Using quadratic growth (a), Theorem 6 in the second step (b), and the choice of T in the following step (c), the iterate x_t with $t \geq T$ satisfies that

$$\|x_t - x_\star\| \stackrel{(a)}{\leq} \sqrt{\frac{1}{\gamma} h_t} \stackrel{(b)}{\leq} \sqrt{\frac{L_f D^2}{\gamma T}} \stackrel{(c)}{\leq} \frac{\delta}{2L_f D}. \quad (43)$$

Next recall the definition of $\mathcal{F}(x_\star)$ implies $(x_\star)_{g_\star} \neq 0$ for any $g_\star \in \mathcal{F}(x_\star)$. The optimality conditions and $\|x_\star\|_{\mathcal{G}} = 1$ (due to $x_\star \in \partial\Omega$) implies that for every $g_\star \in \mathcal{F}(x_\star)$,

$$\langle [\nabla f(x_\star)]_{g_\star}, [x_\star]_{g_\star} \rangle = \|[\nabla f(x_\star)]_{g_\star}\|_* \| [x_\star]_{g_\star} \|, \quad \text{and} \quad \langle \nabla f(x_\star), x_\star \rangle = \|[\nabla f(x_\star)]_{g_\star}\|_*.$$

For any $g_\star \in \mathcal{F}(x_\star)$, define a vector $x_\star^{g_\star} \in \Omega$ as $x_\star^{g_\star} := \begin{cases} \left(\frac{[x_\star]_{g_\star}}{\|[x_\star]_{g_\star}\|} \right)_i, & i \in g_\star, \\ 0, & i \notin g_\star. \end{cases}$ So $x_\star^{g_\star} \in \Omega$ is an

extended vector of the normalized vector $\frac{[x_\star]_{g_\star}}{\|[x_\star]_{g_\star}\|}$. Combining this definition with previous two equalities, we see

$$\langle [\nabla f(x_\star)]_{g_\star}, x_\star^{g_\star} \rangle = \langle \nabla f(x_\star), x_\star \rangle. \quad (44)$$

Now, for any $t \geq T$, we have for any group g_\star in $\mathcal{F}(x_\star)$, and any vector $v \in \Omega$ that is in $\mathcal{F}^c(x_\star)$,

$$\begin{aligned} \langle \nabla f(x_t), x_\star^{g_\star} \rangle - \langle \nabla f(x_t), v \rangle &= \langle \nabla f(x_\star), x_\star^{g_\star} - v \rangle + \langle \nabla f(x_t) - \nabla f(x_\star), v - u \rangle \\ &\stackrel{(a)}{\leq} -\delta + \langle \nabla f(x_t) - \nabla f(x_\star), v - u \rangle \stackrel{(b)}{\leq} -\frac{\delta}{2}. \end{aligned} \quad (45)$$

Here in step (a), we use the definition of δ in (7) and (44). In step (b), we use the bound in (11), Lipschitz continuity of $\nabla f(x)$, and $\|v - u\| \leq D$.

Thus, the k LOO step will produce all the groups in $\mathcal{F}(x_\star)$ as $k \geq r_\star$ after $t \geq T$, and so x_\star is a feasible and optimal solution of the optimization problem in the k direction search step. Hence Algorithm 2 finds the optimal solution x_\star within $T + 1$ steps. \square

B.5 Proofs of Theorem 10

We state one lemma that is critical to our proof of linear convergence. It is proved in Section B.5.1.

Lemma 14. *Given $Y \in \mathbb{R}^{n_1 \times n_2}$ with $\sigma_r(Y) - \sigma_{r+1}(Y) = \delta > 0$. Denote the matrices formed by the top r left and right singular vectors of Y as $U \in \mathbb{R}^{n_1 \times r}$, $V \in \mathbb{R}^{n_2 \times r}$ respectively. Then for any $X \in \mathbb{R}^{n_1 \times n_2}$ with $\|X\|_{\text{nuc}} = 1$, there is an $S \in \mathbb{R}^{r \times r}$ with $\|S\|_{\text{nuc}} = 1$ such that*

$$\langle X - USV^\top, Y \rangle \geq \frac{\delta}{2} \|X - USV^\top\|_{\text{F}}^2.$$

Equipped with this lemma, let us now prove Theorem 10.

Proof of Theorem 10. The case of the spectrahedron is proved in [DFXY20, Theorem 3] by using the eigengap formula in Lemma 11 and [DFXY20, Section 2.2 “relation with the eigengap assumption”]. Here, we need only to address the case of the unit nuclear norm. The proof that we present here for the case of the nuclear norm ball is quite similar. For notation convenience, for each t , let U_t, V_t be matrices formed by top r_\star left and right singular vectors of $\nabla f(X_t)$. Define the set $\mathcal{N}_{r_\star, t} = \{U_t S V_t^\top \mid \|S\|_{\text{nuc}} \leq 1\}$.

First note that Lemma 11 shows that $\delta > 0$. Next, using the Lipschitz smoothness of f , we have for any $t \geq 1$, $\eta \in [0, 1]$, and any $W \in \mathcal{N}_{r_*, t}$:

$$\begin{aligned} f(X_{t+1}) &\leq f(X_t) + (1 - \eta) \langle W - X_t, \nabla f(X_t) \rangle \\ &\quad + \frac{(1 - \eta)^2 L_f}{2} \|W - X_t\|_{\mathbb{F}}^2. \end{aligned} \tag{46}$$

For $t \geq T$, we find that $\|X_t - X_*\|_{\mathbb{F}} \leq \frac{\delta}{6\sqrt{2}L_f}$, and

$$\begin{aligned} &\sigma_{r_*}(\nabla f(X_t)) - \sigma_{r_*+1}(\nabla f(X_t)) \\ &= \underbrace{\sigma_{r_*}(\nabla f(X_*)) - \sigma_{r_*+1}(\nabla f(X_*))}_{\stackrel{(a)}{\leq} -\delta} + \underbrace{(\sigma_{r_*}(\nabla f(X_t)) - \sigma_{r_*+1}(\nabla f(X_*)))}_{\stackrel{(b)}{\leq} \frac{1}{3}\delta} \\ &\quad + \underbrace{(\lambda_{n-r_*+1}(\nabla f(X_*)) - \lambda_{n-r_*+1}(\nabla f(X_t)))}_{\stackrel{(c)}{\leq} \frac{1}{3}\delta} \\ &\leq -\frac{1}{3}\delta. \end{aligned}$$

Here in step (a), we use the singular value gap formula of δ in Lemma 11. Step (b) and (c) are due to Weyl's inequality, the Lipschitz continuity of ∇f , and the inequality $\|X_t - X_*\|_{\mathbb{F}} \leq \frac{\delta}{6\sqrt{2}L_f}$.

Now we subtract the inequality (46) both sides by $f(X_*)$, and denote $h_t = f(X_t) - f(X_*)$ for each t to arrive at

$$\begin{aligned} h_{t+1} &\leq h_t + (1 - \eta) \underbrace{\langle W - X_t, \nabla f(X_t) \rangle}_{R_1} \\ &\quad + \frac{(1 - \eta)^2 L_f}{2} \underbrace{\|W - X_t\|_{\mathbb{F}}^2}_{R_2}. \end{aligned} \tag{47}$$

Using Lemma 14, the inequality (47), and the assumption $X_* \in \partial\Omega$, we can choose $W \in \mathcal{N}_{r_*, t}$ such that

$$\langle W - X_*, \nabla f(X_t) \rangle \leq -\frac{\delta}{6} \|X_* - W\|_{\mathbb{F}}^2. \tag{48}$$

Let us now analyze the term $R_1 = \langle W - X_t, \nabla f(X_t) \rangle$ using (48) and convexity of f :

$$\begin{aligned} R_1 &= \langle W - X_t, \nabla f(X_t) \rangle \\ &= \langle W - X_*, \nabla f(X_t) \rangle + \langle X_* - X_t, \nabla f(X_t) \rangle \\ &\leq -\frac{\delta}{6} \|X_* - W\|_{\mathbb{F}}^2 - h_t. \end{aligned}$$

The term $R_2 = \|X_t - W\|_{\mathbb{F}}^2$ can be bounded by

$$\begin{aligned} R_2 &= \|X_t - W\|_{\mathbb{F}}^2 \stackrel{(a)}{\leq} 2 (\|X_t - X_*\|_{\mathbb{F}}^2 + \|X_* - W\|_{\mathbb{F}}^2) \\ &\stackrel{(b)}{\leq} \frac{2}{\gamma} h_t + 2\|X_* - W\|_{\mathbb{F}}^2, \end{aligned}$$

where we use the triangle inequality and the basic inequality $(a + b)^2 \leq 2a^2 + 2b^2$ in step (a), and the quadratic growth condition in step (b).

Now combining (47), and the bounds of R_1 and R_2 , we reach that there is a $W \in \mathcal{N}_{r_*,t}$ such that for any $\xi = 1 - \eta \in [0, 1]$, we have

$$\begin{aligned} h_{t+1} &\leq h_t + \xi \left(-\frac{\delta}{6} \|X_* - W\|_{\mathbb{F}}^2 - h_t \right) + \frac{\xi^2 L_f}{2} \left(\frac{2}{\gamma} h_t + 2 \|X_* - W\|_{\mathbb{F}}^2 \right) \\ &= \left(1 - \xi + \frac{\xi^2 L_f}{\gamma} \right) h_t + \left(\xi^2 L_f - \frac{\xi \delta}{6} \right) \|X_* - W\|_{\mathbb{F}}^2. \end{aligned}$$

A detailed calculation below and a careful choice of ξ below yields the factor $1 - \min\{\frac{\gamma}{4L_f}, \frac{\delta}{12L_f}\}$ in the theorem.

We show here how to choose $\xi \in [0, 1]$ so that $1 - \xi + \frac{\xi^2 L_f}{\gamma}$ is minimized while keeping $\xi^2 L_f - \frac{\xi \delta}{6} \leq 0$. For $\xi^2 L_f - \frac{\xi \delta}{6} \leq 0$, we need $\xi \leq \frac{\delta}{6L_f}$. The function $q(\xi) = 1 - \xi + \frac{\xi^2 L_f}{\gamma}$ is decreasing for $\xi \leq \frac{\gamma}{2L_f}$ and increasing for $\xi \geq \frac{\gamma}{2L_f}$. If $\frac{\gamma}{2L_f} \leq \frac{\delta}{6L_f}$, then we can pick $\xi = \frac{\gamma}{2L_f}$, and $q(\xi) = 1 - \frac{\gamma}{4L_f}$. If $\frac{\gamma}{2L_f} \geq \frac{\delta}{6L_f} \implies \frac{\delta}{\gamma} \leq 3$, then we can pick $\xi = \frac{\delta}{6L_f}$, and $q(\xi) = 1 - \frac{\delta}{6L_f} + \frac{\delta^2}{36\gamma L_f} = 1 + \frac{\delta}{6L_f} \left(\frac{\delta}{6\gamma} - 1 \right) \leq 1 - \frac{\delta}{12L_f}$. \square

B.5.1 Additional lemmas for the proof of Theorem 10

Here we give a proof of Lemma 14.

Proof of Lemma 14. We utilize the result in [DFXY20, Lemma 5]: given any $\tilde{Y} \in \mathbb{S}^n$ with eigenvalues $\lambda_n(\tilde{Y}) \leq \dots \leq \lambda_{n-r+1}(\tilde{Y}) \leq \lambda_{n-r}(\tilde{Y}) - \delta' \leq \dots \leq \lambda_1(\tilde{Y}) - \delta'$ for some $\delta' > 0$. Denote the matrices by the bottom r eigenvectors of \tilde{Y} as $\tilde{V} \in \mathbb{R}^{n_2 \times r}$ respectively. Then for any $\tilde{X} \in \mathbb{S}_+^n$ with $\mathbf{tr}(\tilde{X}) = 1$, there is an $S \in \mathbb{R}_+^{r \times r}$ with $\mathbf{tr}(S) = 1$ such that

$$\langle \tilde{X} - \tilde{V} S \tilde{V}^\top, \tilde{Y} \rangle \geq \frac{\delta'}{2} \|\tilde{X} - \tilde{V} S \tilde{V}^\top\|_{\mathbb{F}}^2. \quad (49)$$

To utilize this result, we consider the dilation of the matrices X and Y :

$$\tilde{X} := \frac{1}{2} \begin{bmatrix} X_1 & X \\ X^\top & X_2 \end{bmatrix}, \quad \text{and} \quad \tilde{Y} := \begin{bmatrix} 0 & Y \\ Y^\top & 0 \end{bmatrix}. \quad (50)$$

Here the matrices $X_1 = U_X \Sigma_X U_X$, $X_2 = V_X \Sigma_X V_X^\top$ where $U_X \Sigma_X V_X$ is the SVD of X and the number $r_X = \text{rank}(X)$. Since $\tilde{X} = \begin{bmatrix} U_X \\ V_X \end{bmatrix} \Sigma_X [U_X^\top \ V_X^\top]$, the matrix $\tilde{X} \in \mathbb{S}_+^{n_1+n_2} \succeq 0$. The trace of \tilde{X} is $\mathbf{tr}(\tilde{X}) = 1$ as $\|X\|_{\text{nuc}} = 1$. Note that the bottom $r+1$ eigenvalues of \tilde{Y} is simply $-\sigma_1(Y), \dots, -\sigma_r(Y), -\sigma_{r+1}(Y)$, and the matrix $\tilde{V} \in \mathbb{R}^{(n_1+n_2)r}$ defined below is formed by the matrix eigenvectors corresponds the smallest r eigenvalues:

$$\tilde{V} := \frac{1}{\sqrt{2}} \begin{bmatrix} U \\ -V \end{bmatrix}. \quad (51)$$

Using [DFXY20, Lemma 5], we can find a matrix $S \in \mathbb{S}_+^r$ with $\mathbf{tr}(S) = 1$ such that (49) holds. Writing the equation in block form reveals that

$$\langle X - U(-S)V^\top, Y \rangle = \langle \tilde{X} - \tilde{V} S \tilde{V}^\top, \tilde{Y} \rangle \geq \frac{\delta}{2} \|\tilde{X} - \tilde{V} S \tilde{V}^\top\|_{\mathbb{F}}^2 \stackrel{(a)}{\geq} \frac{\delta}{2} \|X - U(-S)V^\top\|_{\mathbb{F}}^2, \quad (52)$$

where the last step is due to Lemma 15. Note that the matrix $U(-S)V^\top$ is the matrix we seek as $\| -S \|_{\text{nuc}} = \mathbf{tr}(S) = 1$. Hence the proof is completed. \square

Lemma 15. *Suppose two matrices $X, Y \in \mathbb{R}^{n_1 \times n_2}$, and $X = U_1 S_1 V_1^\top$ and $Y = U_2 S_2 V_2^\top$ for some unitary U_i, V_i that for some integers r_1, r_2 , they satisfy $U_i \in \mathbb{R}^{n_1 \times r_i}$, $i = 1, 2$ and $V_i \in \mathbb{R}^{n_2 \times r_i}$, $i = 1, 2$. The matrices $S_i \in \mathbb{S}_+^{r_i}$ are positive semidefinite. Then*

$$\|U_1 S_1 U_1^\top - U_2 S_2 U_2^\top\|_F^2 + \|V_1 S_1 V_1^\top - V_2 S_2 V_2^\top\|_F^2 \geq 2\|U_1 S_1 V_1^\top - U_2 S_2 V_2^\top\|_F^2.$$

Proof. This result follows by direct computation. Consider the difference $\|U_1 S_1 U_1^\top - U_2 S_2 U_2^\top\|_F^2 + \|V_1 S_1 V_1^\top - V_2 S_2 V_2^\top\|_F^2 - 2\|U_1 S_1 V_1^\top - U_2 S_2 V_2^\top\|_F^2$. Expanding the square and using the orthogonal invariance of the Frobenius norm, we find that

$$\begin{aligned} & \|U_1 S_1 U_1^\top - U_2 S_2 U_2^\top\|_F^2 + \|V_1 S_1 V_1^\top - V_2 S_2 V_2^\top\|_F^2 - 2\|U_1 S_1 V_1^\top - U_2 S_2 V_2^\top\|_F^2 \\ &= 2\text{tr}(S_1 U_1^\top U_2 S_2 (U_2^\top U_1 - V_2^\top V_1)) + 2\text{tr}(S_1 (V_1^\top V_2 - U_1^\top U_2) S_2 V_2^\top V_1) \\ &\stackrel{(a)}{=} 2\text{tr}(S_1 U_1^\top U_2 S_2 (U_2^\top U_1 - V_2^\top V_1)) + 2\text{tr}(V_1^\top V_2 S_2 (V_2^\top V_1 - U_2^\top U_1) S_1) \\ &\stackrel{(b)}{=} 2\text{tr}(S_1 (U_1^\top U_2 - V_1^\top V_2) S_2 (U_2^\top U_1 - V_2^\top V_1)), \end{aligned}$$

where step (a) is due to the fact that $\text{tr}(A) = \text{tr}(A^\top)$ and step (b) is due to the cyclic property of trace. By factorizing $S_i = S_i^{\frac{1}{2}}$ for $i = 1, 2$ and the cyclic property of trace again, we find that

$$\begin{aligned} & \|U_1 S_1 U_1^\top - U_2 S_2 U_2^\top\|_F^2 + \|V_1 S_1 V_1^\top - V_2 S_2 V_2^\top\|_F^2 - 2\|U_1 S_1 V_1^\top - U_2 S_2 V_2^\top\|_F^2 \\ &= \text{tr}(S_1^{\frac{1}{2}} (U_1^\top U_2 - V_1^\top V_2) S_2^{\frac{1}{2}} S_2^{\frac{1}{2}} (U_2^\top U_1 - V_2^\top V_1) S_1^{\frac{1}{2}}) \\ &= \|S_2^{\frac{1}{2}} (U_2^\top U_1 - V_2^\top V_1) S_1^{\frac{1}{2}}\|_F^2 \geq 0. \end{aligned}$$

Hence the lemma is proved. \square

C Extension for multiple solutions

When the problem has more than one solution, let \mathcal{X} be the solution set. This set is convex and closed. We change the term $\|x - x_\star\|$ in the quadratic growth condition to $\text{dist}(x, \mathcal{X}) = \min_{x_\star \in \mathcal{X}} \|x - x_\star\|$. For strict complementarity, we remove the condition that x_\star is unique and demand instead that some $x_\star \in \mathcal{X}$ satisfies the conditions listed in strict complementarity. The support set $\mathcal{F}(x_\star)$ and complementary set $\mathcal{F}^c(x_\star)$ are defined via the x_\star that satisfies strict complementarity. Note that the dual vector $\nabla f(x_\star)$ is the same for every $x_\star \in \mathcal{X}$ [ZS17, Proposition 1]. The algorithmic results, Theorem 6, 7, and 10 hold almost without any change of the proof using the new definition of r_\star and δ . The argument to establish quadratic growth via strict complementarity is more tedious and we defer it to future work.

D Numerical Experiment setting for Section 4

We detail the experiment settings of Lasso, support vector machine (SVM), group Lasso, and matrix completion problems. The compared methods include FW, away-step FW (awayFW) [GM86], pairwise FW (pairFW) [LJJ15], DICG [GM16], and blockFW [AZHHL17]. All codes are written by MATLAB and performed on a MacBook Pro with Processor 2.3 GHz Intel Core i5 and Memory 8 GB 2133 MHz LPDDR3. In our k-FW, we solve the kDS by the FASTA toolbox [GSB14, GSB15]: <https://github.com/tomgoldstein/fasta-matlab>. In DICG (as well as FW, awayFW, pairFW in Group Lasso and SVM), the step size is determined by backtracking line search. The ball sizes of ℓ_1 norm, group norm, and nuclear norm are set to be the ground truth respectively.

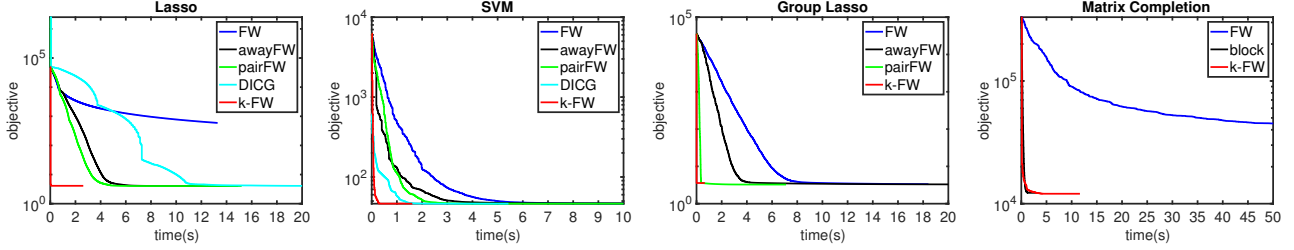


Figure 10: Objective against time cost

D.1 Lasso

The experiment is the same as that in [LJJ15] except that the data size in our setting is ten times of that in [LJJ15]: $A \in \mathbb{R}^{2000 \times 5000}$ and $b \in \mathbb{R}^{2000}$. The large size is more reasonable for comparing the computational costs of FW, awayFW, pairFW, DICG and our k-FW. For FW, awayFW and pairFW, we use the MATLAB codes provide by [LJJ15]: <https://github.com/Simon-Lacoste-Julien/linearFW>. In DICG (as well as FW, awayFW, pairFW in Group Lasso and SVM), the step size is determined by backtracking line search.

D.2 SVM

We generate the synthetic data for two-class classification by the following model

$$X = [X_1 \ X_2] = [U_1 V_1 + 1 \ U_2 V_2 - 1], \quad X \leftarrow X + E,$$

where the elements of $U_1 \in \mathbb{R}^{20 \times 5}$, $V_1 \in \mathbb{R}^{5 \times 500}$, $U_2 \in \mathbb{R}^{20 \times 5}$, and $V_2 \in \mathbb{R}^{5 \times 500}$ are drawn from $\mathcal{N}(0, 1)$. E consists of noise drawn from $\mathcal{N}(0, 0.1\sigma_X)$, where σ_X denotes the standard deviation of the entries of X . Thus, in X , the number of samples is 1000 and the number of features is 20. We use 80% of the data as training data to classify the remaining data. In SVM, we use a polynomial kernel $k(x, y) = (x^\top y + 1)^2$.

D.3 Group Lasso

We generate a 100×1000 matrix X whose entries are drawn from $\mathcal{N}(0, 1)$ and a 10×100 matrix W with 10 nonzero columns drawn from $\mathcal{N}(0, 1)$. Then let $Y = WX$ and set $Y \leftarrow Y + E$, where the entries of noise matrix E are drawn from $\mathcal{N}(0, 0.01\sigma_Y)$. Then we estimate W from Y and X by solving a Group Lasso problem with kFW.

D.4 Matrix Completion

We generate a low-rank matrix as $X = UV^\top$, where the entries of $U \in \mathbb{R}^{500 \times 5}$ and $V \in \mathbb{R}^{5 \times 500}$ are drawn from $\mathcal{N}(0, 1)$. We sample 50% of the entries uniformly at random and recover the unknown entries by low-rank matrix completion.

D.5 Objective function vs running time

See Figure 10. kFW uses considerably less time compared to other FW variants for Lasso, SVM, and Group Lasso problems. It takes longer time than blockFW for the matrix completion problem.